J.-C. Chassaing, C. T. Nitschke, A. Vincenti
(Sorbonne Université)

P. Cinnella
(Laboratoire DynFluid)

D. Lucor
(LIMSI-CNRS)

E-mail:
jean-camille.chassaing@sorbonne-universite.fr

DOI: 10.12762/2018.AL14-07

Advances in Parametric and Model-Form Uncertainty Quantification in Canonical Aeroelastic Systems

Uncertainty quantification is going to play a crucial role in the aeroelastic design and optimization of aircraft. Stochastic aeroelastic models are currently being considered to account for manufacturing tolerance in material properties, variability in flight conditions or uncertainty in the aeroelastic model itself. In this paper, some challenging issues in the development of efficient and robust stochastic solvers are reported within the framework of canonical aeroelastic systems. First, independent or correlated parametric uncertainties are propagated to compute the probability density function of the critical flutter velocity or the limit cycle oscillations in the presence of discontinuous responses. Secondly, inverse stochastic aeroelastic problems are addressed, in which experimental data are used to calibrate several stochastic aerodynamic models within a Bayesian framework. Studied configurations concern linear and non-linear pitching and plunging airfoils, and the stochastic flutter of a cantilevered straight composite wing subject to ply angle and thickness uncertainties.

Introduction

Aeroelasticity can be defined as the study of combined structural and aerodynamic effects on the vibratory behavior of aeronautical components, like panels, wings, rotorcraft or the whole aircraft itself. Aeroelastic effects result from the interaction of inertial, elastic and aerodynamic forces acting on aircraft components. Depending on the aeromechanical properties of the aircraft and the flight conditions, the aeroelastic response may exhibit some undesirable phenomena, ranging from the degradation of the aerodynamic performance of the aircraft to the apparition of self-sustained, possibly dramatic, oscillations of the structure, such as divergence and flutter. Due to the explosive nature of the flutter phenomenon, aircraft certification is mandatory to guarantee that no aeroelastic instability can be encountered inside the flight envelope. However, small variations in the aeromechanical parameters may strongly affect the aeroelastic response of the aircraft [12, 56, 84]. For instance, Thomas *et al.* [103] observed that a 0.10 Hz change in the structural natural frequencies or a 1 deg. change in the mean angle of attack reduce by approximately 10% the computed flutter onset Mach Number.

The study of aeroelasticity with uncertainties, which can be illustrated by using an extension of the classical Collar's aeroelastic triangle of forces (Figure 1), has become an extensive field of research over the last decades [6, 9, 10, 29, 84]. Based on state-of-the-art traditional aeroelasticity and computational aeroelasticity

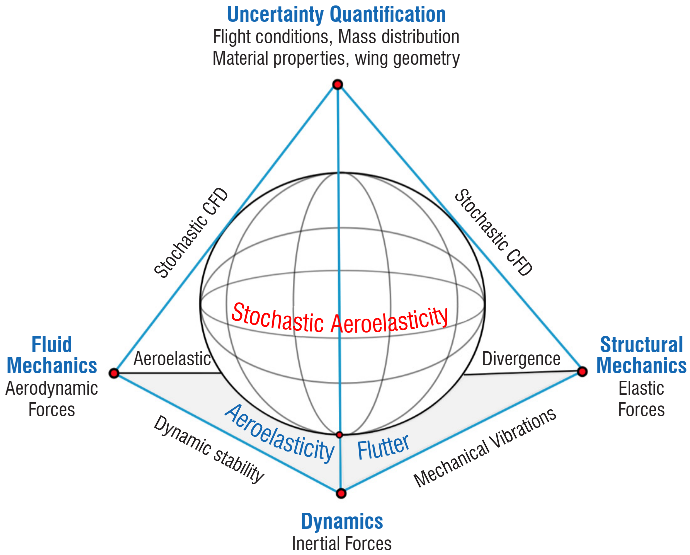

Figure 1 – Probabilistic interpretation of the Collar force triangle in aeroelasticity

approaches [6, 10] originally used within a deterministic framework, uncertainty quantification (UQ) will consist in studying the effect of both aleatory and epistemic uncertainties affecting the aeroelastic response of the aircraft. According to the taxonomy adopted by Melchers [64],any irreducible uncertainty in the system parameters is referred to as aleatory, whereas epistemic uncertainties result from the lack of knowledge about the physical aeroelastic model.

The identification of aeroelastic uncertainties was thoroughly discussed in the review by Pettit [84] on uncertainty quantification in aeroelasticity. Aleatory uncertainties may have various sources, such as, for example, manufacturing tolerance on aircraft geometry or material properties, and in-flight conditions (non-uniform and gusty winds). On the other hand, epistemic uncertainties are typically related to the choice of the physical aeroelastic model. A detailed description of uncertainty sources for physical parameters of aeroelastic configurations can be found in [29].

The study of aeroelasticity with parametric uncertainty can be performed using different approaches. Robust flutter aeroelastic analyses are conducted using non-probabilistic approaches, by studying the stability of the aeroelastic system for parameter variations within given uncertainty bounds. Such approaches, which do not require the probability distribution of the input uncertain aeromechanical parameters, consist in identifying the worst aeroelastic case in the uncertain parametric support [15, 30, 58, 59]. The corresponding methods and advances in the development of non-probabilistic robust aeroelasticity were recently reviewed in [29].

The second type of approach that can be considered to perform aeroelastic studies with uncertainties is referred to as probabilistic aeroelastic analysis. In such a stochastic representation, random input variables with known distributions are used to model the parametric aeroelastic uncertainties. Then, they are propagated using suitable probabilistic approaches, in order to compute the distributions of the aircraft aeroelastic response. The probabilistic collocation methods [5, 100, 124] and the stochastic spectral projection methods [40, 43, 115, 123] are two widely used approaches for the propagation of parametric uncertainty in computational structural dynamics (CSD) and in computational fluid dynamics (CFD). Boosted by the availability of open-source implementations of most popular stochastic solvers [1, 7, 38, 62], CFD-based computations of the stochastic aeroelastic response of elastic structures under uncertain flight conditions or structural variability have been widened substantially [6, 10, 12, 68].

Recently, Stanford and Massey [98] focused on the computation of the failure probabilities of the flexible Common Research Model [109] using a RANS-based CFD solver in the presence of atmospheric, structural and inertial parametric randomness, where up to 11 random variables were considered. In order to deal with a relatively moderate number of random dimensions, a sparse Polynomial Chaos Expansion method (PCE) [45] was used to compute the flutter probability. Although the probability that flutter appears within the commonly adopted 15% flutter margin [2] has been demonstrated at Mach 0.7, PCE fails to accurately compute the tail of the failure probability. It was shown that the lack of accuracy of the spectral projection approach is due to the presence of the physical nonlinearities associated with the transonic regime, which are reported in the random space.

Nowadays, uncertainty quantification in linear and nonlinear aeroelasticity faces several issues that cannot be addressed directly using stochastic approaches like standard PCE and Stochastic Collocation. To this end, there is a need to develop adaptive stochastic approaches in order to deal with a discontinuous response due to the presence of aeroelastic mode switching or subcritical Hopf bifurcations. Moreover, aeroelastic uncertainty quantification studies of realistic configurations involve a large number of random variables, like, for instance, in the case of aircraft components made of composite laminates with uncertain angles and thicknesses in their layup, making the use of adaptive methods more tricky [22]. In order to avoid the development of high-dimensional stochastic solvers, physical low-order modeling can be used to reduce the number of random variables to be propagated, such as, for instance, the use of lamination parameters for the case of the stochastic flutter of a composite wing [94]. However, the resulting uncertainty propagation step must account for correlated random variables, again in the context of possible discontinuity in the random space.

Another major difficulty in the computation of the aeroelastic instability boundary of aircraft is related to the inherent sensitivity of the numerical predictions to the choice of numerical model, as illustrated, for instance, by the difference obtained between the results of Delayed Detached Eddy Simulation and Unsteady Reynolds Averaged Navier-Stokes of the flutter boundary of the AGARD wing 445.6 [125]. In such a context, copying with both parametric and model-form uncertainties in aeroelasticity enables the calibration of uncertain model coefficients from experimental data and, at the same time, the construction of adjusted stochastic models with robust predictive capabilities.

The scope of this paper is to review some recent advances in the development of uncertainty quantification in probabilistic aeroelasticty. Both aleatory and epistemic uncertainties associated with linear and nonlinear canonical aeroelastic systems [21, 52, 77, 78] are considered. Emphasis is placed in Section "Stochastic limit cycle oscillations of the PAPA aeroelastic model" on the treatment of discontinuous response surfaces due to bifurcations in the aeroelastic response of nonlinear PAPA test-cases. The propagation of correlated random variables with arbitrary distributions is described in Section "Stochastic flutter of a composite wing" for the prediction of the stochastic flutter velocity of a composite plate wing.

Finally, the quantification of both model form and parametric uncertainties associated with two low-order aerodynamic models of a PAPA aeroelastic configuration is carried out by using a Bayesian Model Averaging framework.

Forward uncertainty quantification of parametric uncertainties

Stochastic limit cycle oscillations of the PAPA aeroelastic model

Limit cycle oscillations (LCO) can be observed in the presence of nonlinearities in the structural or aerodynamic operator of the aeroelastic system [27, 55, 56]. As illustrated by the typical bifurcation diagram of a PAPA model in Figure 2, the amplitude of these oscillations strongly depends on the subcritical or supercritical nature of the Hopf bifurcation corresponding to a change in the response from a stable solution to an oscillatory behavior [12, 57, 65].

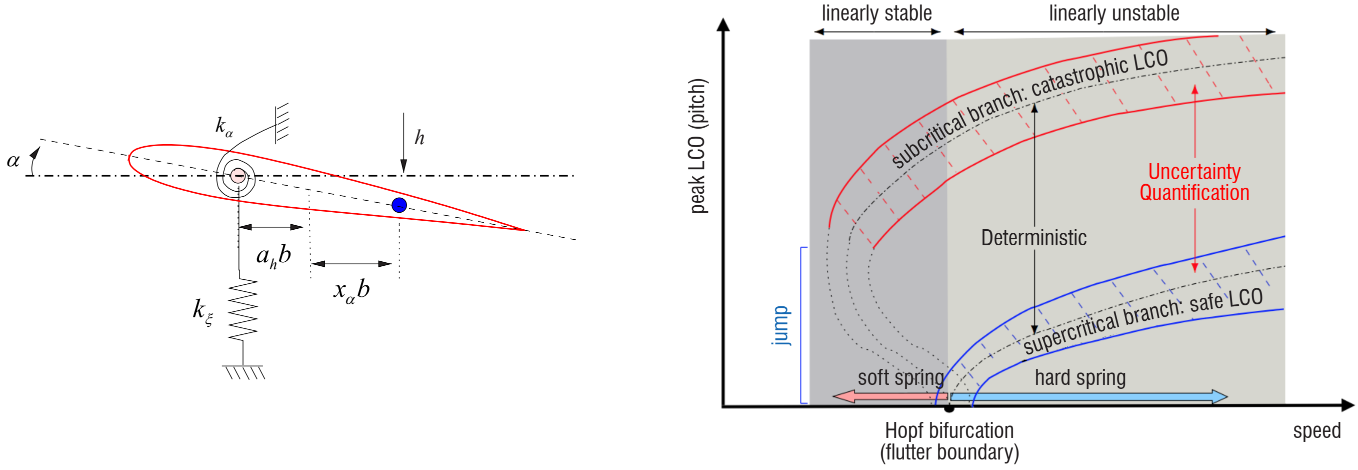

Figure 2 – Left: typical 2DOF pitch and plunge (PAPA) airfoil section problem. Right: Corresponding typical aeroelastic bifurcation diagram due to softening and hardening cubic stiffness restoring forces in pitch.

The onset of LCO of a typical airfoil section model in an incompressible flow with structural nonlinearities in pitch stiffness was studied in a stochastic framework by Pettit and Beran [85]. Subcritical bifurcations were investigated by means of a pentic pitch stiffness model and uncertain initial conditions with Gaussian normal distribution were propagated using Monte Carlo simulations to compute the corresponding stochastic bifurcation diagram. Later, uncertainty quantification in LCO of canonical aeroelastic problems were performed using cheaper stochastic solvers, such as probabilistic collocation methods based on polynomial chaos or Fourier chaos expansions [11, 12, 31, 44, 65, 66, 69, 72, 93, 101, 112], the unsteady adaptive stochastic finite-element approach [116-120] and the stochastic spectral projection [17, 21, 32, 52]. Stochastic LCO and bifurcation diagram of the PAPA canonical aeroelastic model were also investigated in [122] by means of bounded random variables with λ-pdf and in [12] using Wiener-Haar and Wiener-Hermite expansions.

Uncertainty quantification using adaptive spectral methods

The convergence rate of PCE methods with global support may be very slow in the presence of discontinuities in the random space [17, 25, 52, 113, 114, 123], due for instance to a jump from a stable to an unstable aeroelastic response. To circumvent this drawback, the capabilities of the adaptive multi-element generalized Polynomial Chaos (ME-gPC) method developed by Wan and Karniadakis [113] were investigated in [21, 52] for the case of stochastic bifurcation due to non-linear restoring forces in the aeroelastic model.

The first step in the application of the ME-gPC method relies on the definition of an $N-$element partition $\mathbf{D}$ of the random space with B_k elements ($k=1,2,...,N$).

Given a probability space $(\Omega,\mathcal{F},P)$, where Ω is the sample space, $\mathcal{F}$ is a subset of Ω and P is the probability measure, the ME-gPC approximation $u^r(\xi)$ of any space-time random field $u(\boldsymbol{x},t;\boldsymbol{\xi})\in L_2(\Omega,\mathcal{F},P)$ is written as [113]

$$u^r(\xi)=\sum_{k=1}^{N}\sum_{j=0}^{M}\hat{u}_{k,j}\Phi_{k,j}(\xi_k)I_{B_k} \quad (1)$$

where ξ is a random variable defined over the global random space whose components are independent uniform random variables, $\hat{u}_k$ is the local polynomial chaos expansion in element B_k with new random variable ξ_k. The value of the indicator random variable I_{B_k} is equal to 1 when the vector of random variables belongs to element k and is equal to zero otherwise.

The polynomial basis $\{\Phi_{k,j}\}$ is orthogonal in each element with respect to the local probability measure. Then, the gPC coefficients $\hat{u}_{k,j}$ are computed from the Galerkin projection of the stochastic solution onto each member of the local orthogonal basis. The total number of modes M is determined by the dimension d of ξ and the order of the local gPC expansion P is written as $M=((P+d)!)/(P!d!)-1$. Note that, when using uniform/Legendre discretization for the ME-gPC representation, the local polynomials, which must be considered with respect to the conditional probability density function (*pdf*) in each element, remain Legendre polynomials. Therefore, a simple scaling, resulting from the derivation of the conditional *pdf*, is required to map the local element to a standard element of reference.

Although this piecewise polynomial approximation is more appropriate to deal with nonlinear dynamics than the global gPC approach, it must be combined with an adaptive framework in order to avoid computational growth [21, 52, 113]. To this end, a sensitivity-based adaptivity procedure can be constructed starting from the local solution variance obtained from the gPC approximation with polynomial order P.

$$\sigma_{k,p}^2=\sum_{j=1}^{M_P}\hat{u}_{k,j}^2\mathbb{E}\left[\Phi_{k,j}^2\right] \quad (2)$$

Then, coefficients representing the decay rate and the sensitivity to the random dimension can be constructed [113]

$$\eta_k=\frac{\sum_{i=M_{P-1}+1}^{M_P}\hat{u}_{k,i}^2\mathbb{E}[\Phi_{k,i}^2]}{\sigma_{k,p}^2},\quad r_i=\frac{\hat{u}_{i,P}^2\mathbb{E}[\Phi_{i,P}^2]}{\sum_{j=M_{P-1}+1}^{M_P}\hat{u}_j^2\mathbb{E}[\Phi_j^2]},\quad i=1,2,\cdots,d \quad (3)$$

where subscript $\cdot_{i,P}$ denotes the mode consisting only of random dimension ξ_i with polynomial order P.

Finally, the refinement procedure is defined by the following criteria

$$\eta_k^\gamma \Pr\left(I_{B_k}=1\right)\geq\theta_1,\quad r_i\geq\theta_2\cdot\max_{l=1,\cdots,d}r_l \quad (4)$$

where γ, θ_1 and θ_2 are prescribed constant parameters controlling the adaptive procedure. When the first condition is satisfied for element B_k, an anisotropic splitting is performed based on the most sensitive random dimension according to coefficient r_i. Alternatives to this error criterion were proposed by Chouvion and Sarrouy [25], based on the residual error and the local variance discontinuity created by partitioning. In the following sections, the adaptive ME-gPC approach is used to predict the distribution of the LCO amplitude of nonlinear PAPA configurations for both incompressible [52] and supersonic [21] flows in the presence of uncertainties in the torsional restoring stiffness.

Stochastic limit cycle oscillations of a supersonic lifting surface

Lamorte *et al.* [51] used a stochastic collocation approach [36] to propagate variabilities in the pitch and plunge natural uncoupled frequencies of an elastically-mounted 2D supersonic lifting surface. The use of a 6th order expansion with Lagrange polynomials was sufficient to show that under uncertainties, linear flutter may be observed at critical speeds below those obtained under deterministic nominal conditions.

In the following, results obtained about the study of stochastic limit cycle oscillations of an elastically-mounted 2-D supersonic lifting surface (Figure 3) performed using a ME-gPC method [21] are reported.

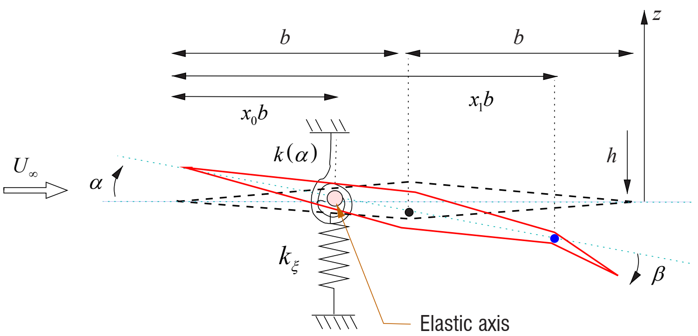

Figure 3 – Two-degree-of-freedom pitch-and-plunge supersonic lifting surface model, with b the half chord, x_α the dimensionless static unbalance and U_∞ the free-stream velocity

The pitch angle α and the dimensionless plunge displacement $\xi = h/b$ of the elastic axis are described by the following canonical aeroelastic equations [57]

$$\begin{aligned} &\xi'' + x_\alpha \alpha'' + 2\zeta_h \frac{\varpi}{V}\xi' + \left(\frac{\varpi}{V}\right)^2 \xi = l_a(\tau) \\ &\frac{x_\alpha}{r_\alpha^2}\xi'' + \alpha'' + 2\frac{\zeta_\alpha}{V}\alpha' + \left(\frac{1}{V}\right)^2 k(\alpha) = -m_a(\tau) \end{aligned} \quad (5)$$

The non-dimensional lift $l_a(\tau)$ and aerodynamic pitching moment $m_a(\tau)$, which account for the flap deflection angle β, are computed using an unsteady nonlinear aerodynamic model based on the piston theory in the third approximation [57]. The complete description of the dimensionless aero-mechanical parameters r_α, μ, ζ_α, ζ_ξ, ϖ, $k(\alpha)$ can be found in [54]. The nondimensional airspeed parameter is V and the primes refer to differentiation with respect to the nondimensional time $\tau = U_\infty t/b$ (Figure 3). The aeroelastic equations can be written in space-state form as [21]

$$\dot{\mathbf{x}} = \mathbf{A}\mathbf{x} + \left(\mathbf{p}_s + \mathbf{p}_a\right)\alpha^3 + \mathbf{f} \quad (6)$$

where the state vector $\mathbf{x} = \left[\xi \quad \alpha \quad \xi' \quad \alpha'\right]^T$ is obtained using an explicit fourth-order Runge-Kutta time-integration scheme. [54]

As discussed in the introduction, it is well known that physical nonlinearities in the restoring forces may promote sharp and sudden flutter onset for small changes in the reduced velocity. The purely deterministic parametric investigations conducted in [86] were revisited within a stochastic framework using the ME-gPC approach in [21]. To this end, the structural damping coefficients ζ_h and ζ_α (Equation 6) are considered as input variables with an independent *uniform* random distribution:

$$\begin{aligned} \zeta_h &= \bar{\zeta}_h + \sigma_{\zeta_h}\Theta_1 \\ \zeta_\alpha &= \bar{\zeta}_\alpha + \sigma_{\zeta_\alpha}\Theta_2 \end{aligned} \quad (7)$$

where $\bar{\zeta}_h = \bar{\zeta}_\alpha = 0.005$ and $\sigma_{\zeta_h} = \sigma_{\zeta_\alpha} = 0.005$.

The response surface of the pitch amplitude obtained for a Mach number of 2.1 using a global gPC representation with a relatively high polynomial order $P = 14$ is shown in Figure 4-left.

Spurious oscillations of the response surface are clearly visible for both the stable state and the LCO branch. The global gPC response surface fails to clearly identify the discontinuity front in the random space, resulting in a poor representation of the stochastic response.

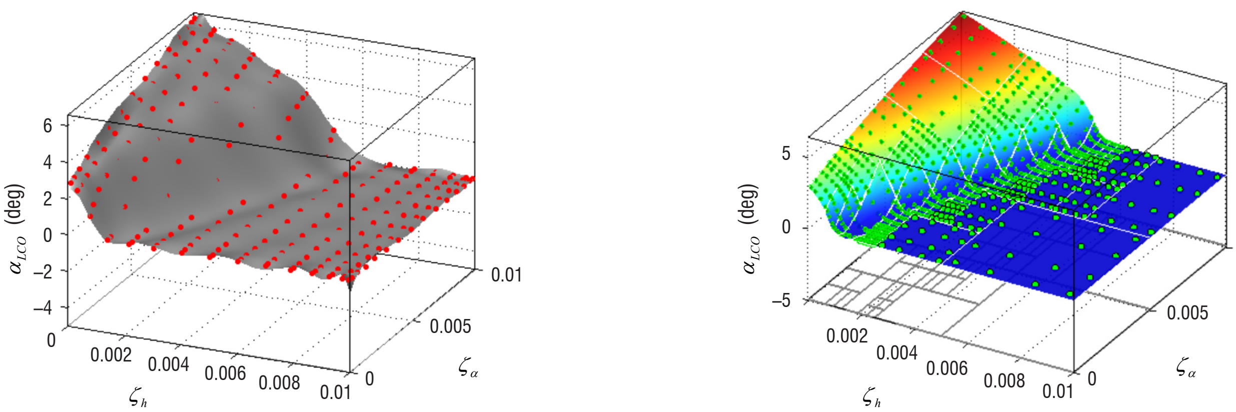

Figure 4 – Left: gPC response surface of α_{LCO} at $M = 2.1$ obtained using polynomial order $P = 14$. Right: ME-gPC results. The deterministic aeromechanical parameters are [21]: $x_\alpha = 0.25$, $r_\alpha = 0.5$, $b = 1.5$, $\varpi = 1$, $\mu = 50$, $x_0 = 0.5$, $\mu = 50$, $\gamma = 1.4$, $B = 5$

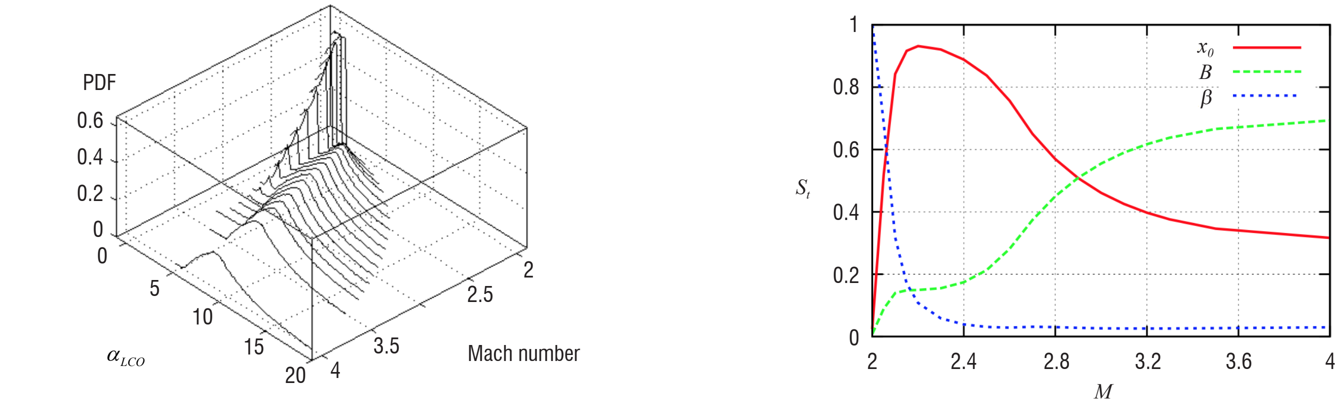

Figure 5 – Left: Distributions of the pitch LCO amplitude α_{LCO} obtained for $M=2$ up to $M=4$ for randomness due to the elastic axis location x_0, the nonlinear torsional stiffness parameter B and flap angle β. Right: Stochastic sensitivity study using Total Sobol indices in the case of three sources of randomness in x_0, B and β [21]

Due to a refinement process performed according to the most sensitive random dimensions (Equation 3), the ME-gPC expansion with $P=3$ succeeds in accurately capturing the steep front in the response, where 8 grid-levels were required to reach a resolution level set to $\varepsilon_1=10^{-3}$. The total number of cubature points required by the piecewise gPC solver is 1456 (encompassing 55 elements) compared to $(P+1)^2=225$ points for the global gPC representation.

In the following, parametric uncertainties in the elastic axis location, the nonlinear torsional stiffness parameter and flap angle are propagated using the ME-gPC approach. Figure 5-left shows the *pdf* of pitch LCO computed for operating conditions ranging from Mach number $M=2$ up to $M=4$. Each distribution is estimated from the ME-gPC expansions using 1 million samples. The bimodal shape of the distribution of the peak LCO, visible up to $M=2.8$, corresponds to the stochastic bifurcation region. The stable stationary branch is characterized by a *uniform*-like distribution with possible pitch amplitude ranging between 0 and 2 deg. We remark that the shape of the distribution is not strongly influenced by the Mach number in the post-bifurcation region defined by $M>3$. However, the upper limit of possible values of the peak pitch amplitude exhibits a nonlinear behavior according to the Mach number.

The analysis of the stochastic solution sensitivity to the uncertain parameters can be performed by means of the *total* Sobol indices [96], which are computed *a posteriori* using two independent MC sample sets drawn from the piecewise gPC expansion [21]. As shown in Figure 5-right, the most sensitive random variable differs depending on flow conditions. The lower bound of the Mach number range ($M<2.1$) is dominated by randomness in the flap angle. However, the stochastic solution in the bifurcation region ($M\in[2.1,2.9]$) is sensitive to inherent variations in the position of the elastic center. Conversely, uncertainties in both the nonlinear stiffness term and the location of the elastic axis mainly affect the stochastic response for high Mach numbers ($M>2.9$).

Subcritical stochastic bifurcation with random initial pitch angle and cubic spring term

The ME-gPC approach was successfully used in [52] to predict stochastic bifurcations with *uniformly* distributed random inputs in the linear torsional stiffness coefficient ($\bar{k}_{\alpha_1}=1$ and $\sigma_{k_{\alpha_1}}=0.1$) and the cubic torsional stiffness coefficient ($\bar{k}_{\alpha_3}=3$ and $\sigma_{k_{\alpha_3}}=0.75$) of a PAPA canonical model for incompressible flows. The pdf isocontours of the LCO amplitude in pitch α_A (Figure 6-right) reveal that three distinct regions can be identified in the stochastic aeroelastic response of the airfoil: (i) damped oscillations for $U^*<6.6$, (ii) a bi-modal response in the bifurcation region with both damped oscillations and LCO and (iii) a post-bifurcation region for $U^*>6.6$. Moreover, the error bars of the prediction of α_A (Fig. 6-left) show that, in the presence of combined uncertainties in k_{α_1} and k_{α_3}, the instability onset could appear before the nominal (deterministic) flutter conditions are reached.

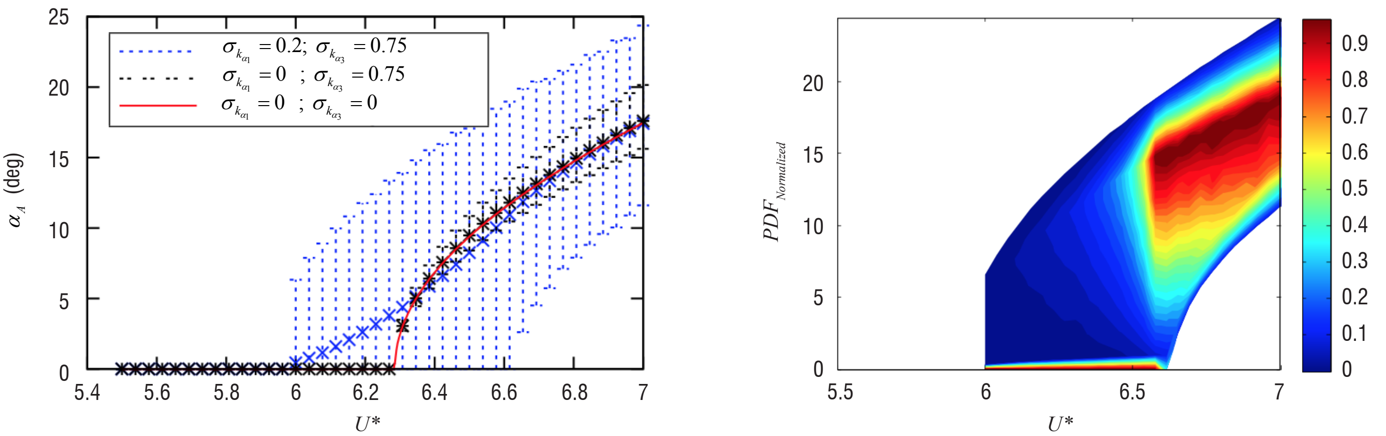

Figure 6 – Distribution of the amplitude LCO branch due to cubic hardening stiffness in pitch [52]

Figure 7 shows a subcritical stochastic bifurcation obtained for uncertainties in the initial pitch angle $\alpha(0)$ and cubic spring term k_{α_3}. The distribution of the peak pitch amplitude due to statistic of these uncertain variables defined by $\bar{\alpha}(0)=12.5$ deg, $\sigma_{\alpha}(0)=12.5$ deg, $\bar{k}_{\alpha_3}=-3$ and $\sigma_{k_{\alpha_3}}=0.75$ are presented in Figure 7-left. The stochastic bifurcation regime is studied for reduced velocities ranging from $U^*=5.8$ to $U^*=6.3$. The bimodal density response of the peak LCO amplitude in pitch corresponds to a sharp Dirac delta-like peak due to the zero-amplitude stable branch and a second peak corresponding to the probability to observe the stable large amplitude LCO branch, which results from the discontinuous shape of the response surface, as shown in Figure 7-mid for $U^*=6$.

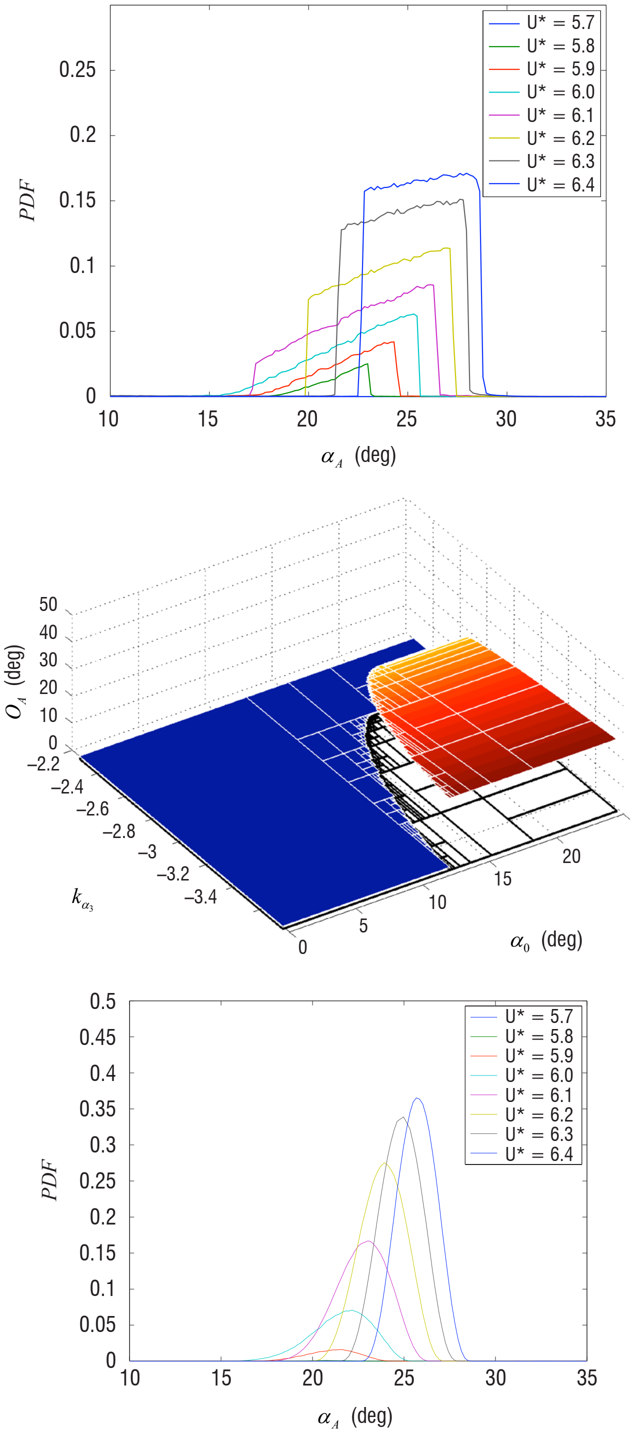

Figure 7 – Up: pdf of the stable large amplitude LCO branch due to uncertainties in $\alpha(0)$ and k_{α_3} described by uniform distributions. Mid: corresponding ME-gPC response surface computed for $U^*=6$. Bottom: distribution of α_{LCO} assuming the k_{α_3} and $\alpha(0)$ follow independent $Beta(\alpha=3,\beta=3)$ distributions [52]

Although the previous stochastic study was performed using *uniformly* distributed inputs, it is possible to compute the stochastic response due to different random input distributions defined on the same support of the probability space [52]. In this case, the statistics of the response can be readily obtained as a post-processing stage using Equation 1. As an example, Figure 7-right shows the shape of *pdf* of α_{LCO} obtained when both k_{α_3} and $\alpha(0)$ follow independent $Beta(\alpha=3,\beta=3)$ distributions. Although the resulting distributions of the peak pitch amplitude look similar to $Beta$ distributions, the tails of the distribution exhibits a longer left tail toward the zero-amplitude stable branch.

Stochastic flutter of a composite wing

Global-support-based Polynomial-Chaos expansions were used by Manan and Cooper [61] for the propagation of uncertain longitudinal Young modulus and shear modulus in the frequency response function of a composite wing. Recently, Scarth *et al.* [94] addressed the problem of uncertainty quantification in the ply angle uncertainty of a composite rectangular wing. To this end, the composite laminate layups were modeled using the lamination parameters [106], in order to reduce the number of random dimensions of the stochastic problem. Rosenblatt decomposition was applied to deal with correlations in the input random variables. Moreover, a convex-hull approach was considered in order to split the random domain, according to the discontinuity due to the presence of a mode switch in the aeroelastic response of the composite wing. This approach was successfully used to capture the multi-modal response of the distribution of the critical flutter velocity, whereas results obtained using a Polynomial Chaos Expansion with global support are not sufficiently accurate. However, the aeroelastic configurations of interest were concerned with uncertainties in ply angles only and the effects of membrane-bending coupling were neglected, thus introducing an artificial symmetrization of the material in the stochastic framework.

In this section, we consider the study of uncertainty propagation on the linear flutter speed of a composite cantilevered wing due to parametric variabilities in the angular ply placement and thickness for several laminate configurations [73, 78]. Since laminates with a dozen or more plies can be used in aeronautical components, the corresponding number of uncertain constitutive parameters is expected to be large compared to those of the stochastic study in Section "Stochastic limit cycle oscillations of the PAPA aeroelastic model". Therefore, we introduce the polar method [108, 111] as a possible way to reduce the random dimensional space. As a side effect, conventional spectral projection methods must be adapted to deal with correlated random variables and arbitrary input distributions.

Aeroelastic system

We aim to investigate the stochastic aeroelastic response of a flat cantilevered laminated composite plate [94, 99] depicted in Figure 8. The wing geometry is reported in Table 1.

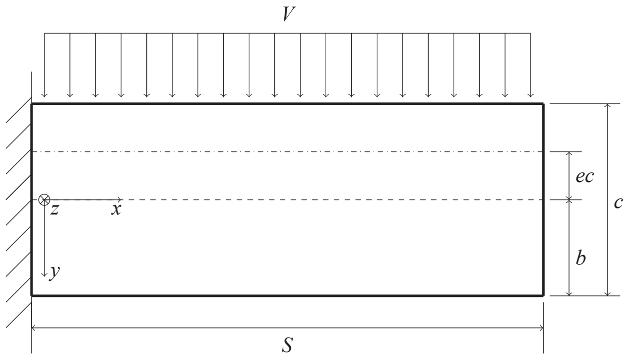

Figure 8 – Scheme of the studied cantilevered laminated plate wing [99]

Wing half span $S[m]$	Chord $c[m]$	Air density $\rho_a\left[kg/m^3\right]$	Lift excentricity e	Unsteady parameter $M_{\dot{\theta}}$
0.3048	0.0762	1.225	0.25	–1.2

Table 1 – Wing geometry and aeromechanical data [99]

Hereafter, we consider sixteen-layer layups based on AS4/3502 graphite/epoxy laminate [106, 107], and the engineering moduli of this base layer are summarized in Table 2.

$E_1[GPa]$	$E_2[GPa]$	$G_{12}[GPa]$	$\nu_{12}[-]$	$\rho\left[kg/m^3\right]$	Ply thickness $t[mm]$
138.0	8.96	7.1	0.3	1600	0.1

Table 2 – Material properties of AS4/3502 UD layer

In the absence of membrane forces, the bending moments m are related to the curvature $\boldsymbol{\kappa}=\left(-\frac{\partial^2 w}{\partial x^2},-\frac{\partial^2 w}{\partial y^2},-2\frac{\partial^2 w}{\partial x \partial y}\right)^T$ by

$$\mathbf{m}=\left(\mathbf{D}-\mathbf{B}\mathbf{A}^{-1}\mathbf{B}\right)\boldsymbol{\kappa}=\tilde{\mathbf{D}}\boldsymbol{\kappa} \tag{8}$$

where $\mathbf{A}$ denotes the membrane stiffness, $\mathbf{D}$ is the bending stiffness, $\mathbf{B}$ describes the coupling between the membrane and the bending forces, and $\tilde{\mathbf{D}}$ is the modified bending stiffness [67], which reduces to tensor $\mathbf{D}$ for uncoupled laminates.

The aeroelastic governing equations are obtained using the Lagrange equations for the generalized coordinates $\mathbf{q}$

$$\frac{d}{dt}\left(\frac{\partial T}{\partial \dot{\mathbf{q}}}\right)-\frac{\partial T}{\partial \mathbf{q}}+\frac{\partial U}{\partial \mathbf{q}}=\frac{\partial(\delta W)}{\partial(\delta \mathbf{q})} \tag{9}$$

where the potential energy U, the kinetic energy T and the virtual work of the aerodynamic forces are

$$\begin{aligned} U &= \frac{1}{2}\iint \boldsymbol{\kappa}^{\mathrm{T}}\tilde{\mathbf{D}}\boldsymbol{\kappa}\,dxdy \\ T &= \frac{1}{2}\rho d\iint \dot{w}^2 dxdy \\ \delta W &= \int l_a(-\delta w)dx+\int m_a \delta\theta dx \end{aligned} \tag{10}$$

As in the work by Stodieck *et al.* [99], the quasi-steady strip theory [121] was used to model the aerodynamic lift l_a and moment m_a [99].

The governing equations are solved using a Rayleigh-Ritz approximation of the displacements w, which are represented by a combination of algebraic polynomials. The resulting equations of motion are written as the following generalized eigenvalue problem [78] in terms of the vector $\hat{\mathbf{q}}$ of the $n_x \times n_y$ amplitude coefficients $\hat{q}_{(ij)}$

$$\begin{bmatrix} 0 & \mathbf{I} \\ \left(\mathbf{K}_{aero}-\mathbf{K}_{struct}\right) & \mathbf{D}_{aero} \end{bmatrix}\begin{bmatrix} \hat{\mathbf{q}} \\ \lambda\hat{\mathbf{q}} \end{bmatrix}=\begin{bmatrix} \mathbf{I} & 0 \\ 0 & \mathbf{M}_{struct} \end{bmatrix}\lambda\begin{bmatrix} \hat{\mathbf{q}} \\ \lambda\hat{\mathbf{q}} \end{bmatrix} \tag{11}$$

where $\mathbf{M}_{struct}$, $\mathbf{D}_{aero}$, $\mathbf{K}_{aero}$ and $\mathbf{K}_{struct}$ are respectively, the structural mass matrix, the aerodynamic damping matrix, the aerodynamic stiffness matrix and the elastic stiffness matrix.

The critical flutter conditions are defined by $\mathfrak{Re}(\lambda)=0$ with corresponding flutter speed V_f and circular frequency ω_f. Details about the aeroelastic solver can be found in [73].

Random variable reduction using the Polar Method

The concept of lamination parameters [106] and polar method [108, 111] are two widely used approaches for the analysis and design of composite laminates. They provide a smaller set of parameters to describe the behavior of a laminate instead of considering the entire set of constitutive parameters. Therefore, they are particularly suited for propagating uncertainties in layer thicknesses and angles due to the manufacturing process, by reducing the number of random variables, thus making possible the use of the Polynomial-Chaos-based spectral projection method, for instance. Due to its natural ability to deal with uncertainty in ply thickness and its natural physical meaning, the polar method, which is based on tensor invariants was recently used by Nitschke *et al.* [73, 78] in the context of aeroelastic UQ of composite plates.

The polar method consists in describing the modified bending tensor $\tilde{\mathbf{D}}$ by the polar constants $\boldsymbol{\theta}=\left\{T_0^{\tilde{D}},T_1^{\tilde{D}},R_0^{\tilde{D}},R_1^{\tilde{D}},\Phi_0^{\tilde{D}},\Phi_1^{\tilde{D}}\right\}$, such as [108, 111]

$$\begin{aligned} \tilde{D}_{xx} &= T_0+2T_1+R_0\cos\left(4\Phi_0\right)+4R_1\cos\left(2\Phi_1\right) \\ \tilde{D}_{xy} &= -T_0+2T_1-R_0\cos\left(4\Phi_0\right) \\ \tilde{D}_{xs} &= R_0\sin\left(4\Phi_0\right)+2R_1\sin\left(2\Phi_1\right) \\ \tilde{D}_{yy} &= T_0+2T_1+R_0\cos\left(4\Phi_0\right)-4R_1\cos\left(2\Phi_1\right) \\ \tilde{D}_{ys} &= -R_0\sin\left(4\Phi_0\right)+2R_1\sin\left(2\Phi_1\right) \\ \tilde{D}_{ss} &= T_0-R_0\cos\left(4\Phi_0\right) \end{aligned} \tag{12}$$

where quantities T_0,T_1,R_0,R_1 and $\left(\Phi_0-\Phi_1\right)$ are invariants. The isotropic part of the tensor is represented by parameters T_0 and T_1, coefficients R_0 and R_1 are the modules of the anisotropic part and Φ_0 and Φ_1 are the corresponding orientation angles.

Figure 9 presents the flutter response of the studied cantilevered wing (Table 1) over the polar domain of nominally orthotropic and uncoupled laminates and considering that the principal orthotropy axis of the laminate is aligned with the wing mid-chord axis.

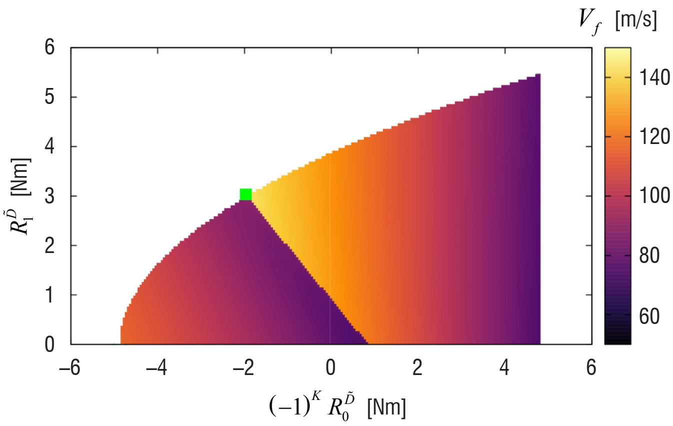

Figure 9 – Response surface of the critical flutter speed V_f defined in the polar domain for orthotropic laminates [78] for the cantilevered plate wing (Figure 8). The green dot corresponds to the configuration depicted in Table 3 and giving the maximum flutter speed.

We immediately remark a step in the critical flutter speed V_f, which separates the response surface into two sub-regions. This discontinuity illustrates the mode switch present in the aeroelastic instability mechanism of the studied configuration. We also note that the laminate configurations corresponding to the extreme values of V_f (V_f^{max}=148.5 m/s and V_f^{min} =76.3 m/s) are very close, approximately in the region close to the point $(-1)^K R_0^D$ = −1.948 and R_1^D = 3.032 (green dot in Figure 9) apart from the step. This fact, clearly illustrates the need for considering uncertainties in the aeroelasticity analysis, since tolerance errors in the elastic stiffness of the composite laminate, due for instance to the manufacturing process, could lead to the worst flutter case, whereas it is designed to be the best flutter case within a deterministic framework.

In the following, we consider the layup configuration, which maximizes the flutter speed (see the green dot in Figure 9). The corresponding polar properties and stacking sequence are reported in Tables 3 and 4, respectively.

Next, we consider randomness in the ply angles and thicknesses, according to a Gaussian distribution with standard deviation of 1 [°] and 0.005 [mm] respectively. These parametric uncertainties in the sixteen-layer layup are propagated by Monte Carlo simulation, in order to characterize the *pdf* of the six polar constants (Equation 12). As illustrated by the scatter plot of $R_1^{\tilde{D}}$ against $T_0^{\tilde{D}}$ in Figure 10-left, the polar constants exhibit rather strong correlations depending on the configuration of the layup. Moreover, the resulting distributions no longer have a Gaussian shape, and they can be arbitrary symmetric or skew distributions, as shown in Figure 10-mid/right.

The fact that the random variables of the polar constants are not independent, with non-Gaussian distributions, is due to the nonlinear nature of the transformation in Equation 12. Therefore, the uncertainty quantification in the ply angles and thicknesses by means of polar constants requires conventional global-Polynomial-Chaos stochastic solvers to be adapted, in order to deal with (i) arbitrary input distributions, (ii) correlated random variables and (iii) discontinuity in the random space.

The first two points are addressed by using the arbitrary Polynomial Chaos method (aPC) presented in [70, 79, 82, 97, 120]. The latter point was treated by combining the aPC approach with machine-learning techniques, in order to identify clusters of points belonging to each sub-region of the response surface.

$T_0^{\tilde{D}}[Nm]$	$T_1^{\tilde{D}}[Nm]$	$(-1)^K R_0^{\tilde{D}}[Nm]$	$R_1^{\tilde{D}}[Nm]$	$\Phi_0^{\tilde{D}}[^\circ]$	$\Phi_1^{\tilde{D}}[^\circ]$	$V_f[m/s]$	$\omega_f\left[\frac{rad}{s}\right]$
7.288	6.538	−1.948	3.032	0	0	143.48	505.24

Table 3 – Polar properties and flutter response of the studied configuration, which corresponds to the maximum flutter speed $V_{f_{max}}$ in the response surface (Figure 9)

Stacking sequence	Property summary
[28.4$_2$, −28.4$_4$, 28.4$_2$, −28.4$_2$, 28.4$_4$, −28.4$_2$]	general orthotropic, $V_{f_{max}}$

Table 4 – Stacking sequence of the AS4/3502-based laminate corresponding to parameters given in Table 3

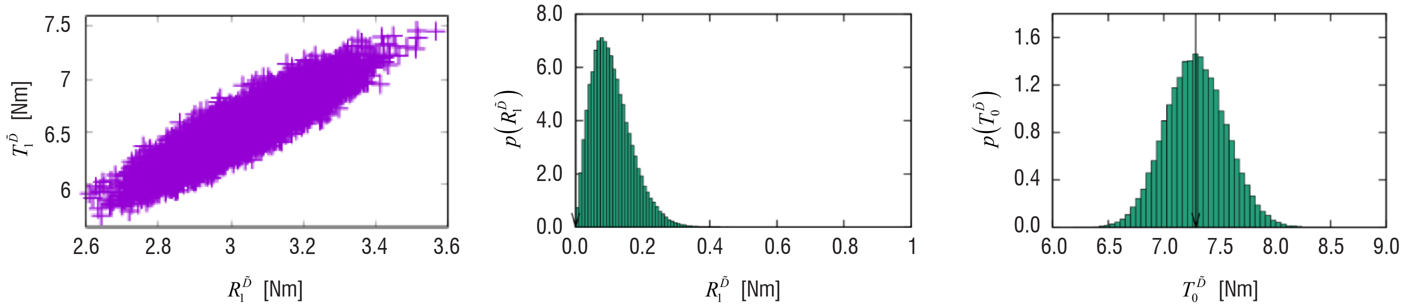

Figure 10 – Scatter plots and distributions of modified bending polar parameters $R_1^{\tilde{D}}$ and $T_0^{\tilde{D}}$ due to uncertainties in angular ply placement and thickness based on the nominal configuration of the composite laminates in Table 3 [78]

Dealing with correlations in the random polar parameters

As seen in Section "Uncertainty quantification using adaptive spectral methods", the spectral expansion in the stochastic space of the Polynomial Chaos methods relies on the use of the orthogonal polynomial basis Φ_i and expansion coefficients $\hat{u}_i$ (Equation 1). In order to be able to deal with arbitrary distributions and correlated variables, we follow the work by Navarro *et al.* [70, 120], in which a Gram-Schmidt algorithm is used to compute the coefficients of the polynomials based on the scalar product

$$\left\langle \phi_i, \phi_j \right\rangle = \int_{\Theta} \phi_i(\boldsymbol{\theta}) \phi_j(\boldsymbol{\theta})\, p(\boldsymbol{\theta})\, d\boldsymbol{\theta} = \mathbb{E}\left\{ \phi_i(\boldsymbol{\theta})^2 \right\} \delta_{ij} \qquad (13)$$

Since no analytical representation of the joint distribution of the random polar constants is available, the integrals required for the computation of the coefficients of polynomials are derived from MC integration based on the analytical expression of the polar parameters in Equation 12. Moreover, a least-square fitting procedure is used to compute the expansion coefficients $\hat{u}_i$, based on MC draws in the random space. The extension of the aPC method to correlated random variables is detailed in [78].

UQ in the vicinity of the aeroelastic mode switch

In Section "Stochastic limit cycle oscillations of a supersonic lifting surface", the ME-gPC method was used to deal with discontinuities in the random space. Here, an alternative method is developed by combining the global support aPC solver with a machine learning-based filtering procedure in order to decompose the response surface according to different aeroelastic modal regimes. Note that Scarth *et al.* [94] have addressed the same aeroelastic problem by coupling the gPC method with the Rosenblatt transformation and convex hull identification for response surface splitting.

The present approach consists of two steps [73, 78]. First, the different modal regimes in the response surface are identified by applying the DBSCAN clustering algorithm [37] from a preliminary set of samples of the flutter speed V_f and frequency ω_f, requiring typically 10^3 calls to the aeroelastic solver.

Figure 11-left illustrates the identification step of the modal regimes due to the uncertainties defined in Section "Random variable reduction using the Polar Method", from the laminate presented in Table 3 and whose nominal configuration maximizes the flutter speed (green square symbol in Figure 9). Based on the preliminary sampling of V_f and ω_f, the DBSCAN algorithm succeeds in clustering the data as shown by the different colors of the clouds. The number of samples used in the aPC.

In the second step, a large set of samples of polar parameters, drawn from their analytical expression (Equation 12), are used (typically with size of 10^5), in conjunction with the training data from the clustering, by a neural network-type Multi-layer perceptron classifier [83], in order to generate filtered samples that are used for the construction of the polynomials in the aPC solver for each sub-region of the discontinuous response surface. Moreover, the fitting procedure in the aPC is performed using the clustered samples, thus avoiding any additional calls to the aeroelastic solver. Details about the implementation of the machine-learning approach used within the context of the aeroelastic aPC framework are given in [78].

The multi-modal aPC-machine learning classifier method was used to compute the distribution of the flutter speed shown in Figure 11-right for nominal conditions giving the maximum flutter speed. As expected, the bi-modal shape of the distribution relies on the mode switch as a consequence of randomness in the ply angles and thicknesses. The peak at high critical flutter speed is located near the nominal value $V_f = 143\, m/s$. The lower peak appears for a critical flutter speed around $V_f = 83\, m/s$. It is clear that, in the present case, the conventional flutter margin of $122\, m/s$, which corresponds to a 15% offset from the nominal value, fails to define a safety operational range, as confirmed by the computation of the 1% percentile (Figure 11-right).

Note that the comparison of the distribution of V_f with a Monte Carlo simulation shows that the present multi-modal aPC approach could be an interesting approach to propagate correlated parametric uncertainties with arbitrary input distribution in the presence of discontinuity in the random space.

Model-form uncertainty quantification in aeroelasticity

Although it was previously shown that parametric uncertainties can be efficiently propagated through an aeroelastic model to predict the stochastic response of the critical flutter speed or LCO amplitudes, epistemic uncertainties, which result from a lack of knowledge, may induce greater variability in the stochastic response than real physical randomness [103, 126]. Therefore, the quantification of model assumptions and predictive uncertainties [26, 81] should be taken into account in the prediction of the stochastic aeroelastic response.

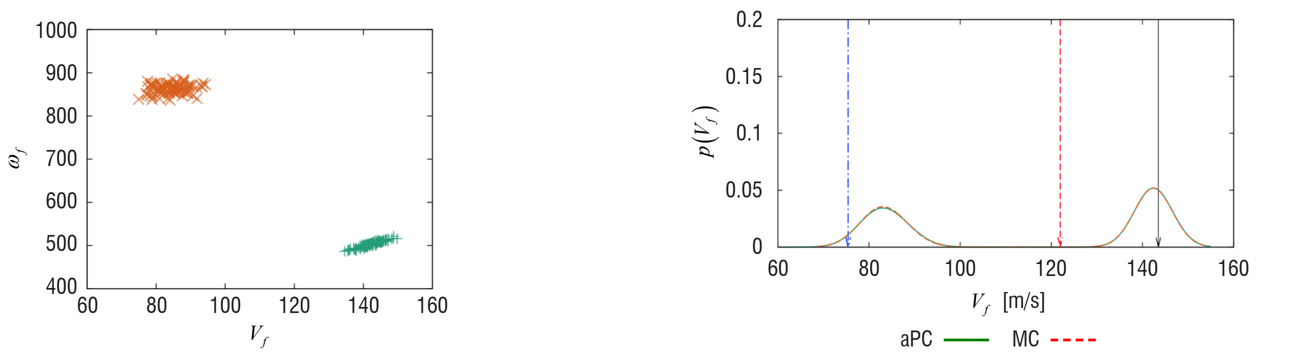

Figure 11 – Aeroelastic uncertainty propagation in ply angles and thicknesses of the sixteen-layer AS4/3502 graphite/epoxy laminate (Table 3). Left: Clouds of samples showing V_f plotted against ω_f and colored by the results of the DBSCAN clustering. Right: Multi-modal distribution of the flutter speed V_f computed using the machine learning augmented aPC method [79]. The solid black arrow indicates the nominal critical flutter speed, the red dashed arrow is the classical 15% flutter margin and the blue dash-dotted arrow indicates the 1% percentile for the occurrence of flutter.

Number of states	Reference	Function definition
Two states	Jones R.T [46]	$C(k) \approx 1.0 - \frac{0.165k}{k-0.0455i} - \frac{0.335k}{k-0.3i}$
	Jones W.P [47]	$C(k) \approx 1.0 - \frac{0.165k}{k-0.041i} - \frac{0.335k}{k-0.32i}$
	Riley [89]	$C(k) \approx \frac{(1.0+10.61ik)(1.0+1.774ik)}{(1.0+13.51ik)(1.0+2.745ik)}$
	Jones rounded [89]	$C(k) \approx \frac{0.015+0.3ik-0.5k^2}{0.015+0.35ik-k^2}$
Four states	Brunton [18]	$C(k) \approx \frac{0.5k^4-0.703ik^3-0.2393k^2+0.01894ik+2.32510^{-4}}{k^4-1.158ik^3-0.3052k^2+0.02028ik+2.32510^{-4}}$
	Vepa [110]	$C(k) \approx \frac{k^4-0.761ik^3-0.1021k^2+2.551i10^{-3}k+9.55710^{-6}}{2k^4-1.064ik^3-0.1134k^2+2.617i10^{-3}k+9.55710^{-6}}$

Table 5 – Approximations of the Theodorsen function used to construct the stochastic lift functions [75].

Typically, the choice of low- or high-fidelity structural and aerodynamic operators to be considered for aeroelastic simulations relies on model-form uncertainty, with possible uncertain parameters, which may strongly affect the prediction of the flutter boundary. Another important issue concerns the sensitivity of these models, which may strongly differ depending on the physical scenario of interest.

Such stochastic problems can be addressed using Bayesian inference methods for parameter calibration and model updating, as in [4, 16, 53]. First, a likelihood function must be built, based on prescribed prior distributions of model coefficients and observations of parameters of interest. Then, the Bayes theorem is applied to compute the joint posterior distribution of model parameters using Markov Chain Monte Carlo (MCMC) sampling. In this case, an adjusted stochastic model can be constructed using the Bayesian Model Averaging Approach (BMA) [42], where previously individual calibrated models are weighted using their posterior model probability.

A Bayesian estimation of structural uncertainties of the Goland wing was performed by Dwight *et al.* [35], in whose work the use of few observation data was sufficient to substantially reduce the variability in the parameters of the high-fidelity CFD/Finite Element aeroelastic solver. A BMA adjusted statistical model dedicated to the computation of the flutter margin of the 445.6 wing was deployed by Riley and Grandhi [88]. The same aeroelastic configuration was used by Riley [89] to predict both model-form and parametric uncertainties in the flutter margin, where the latter are propagated using the fast Fourier transform technique with a weighted-Stack Response Surface method.

Intensive research in the field of Bayesian parameter estimation for nonlinear aeroelasticity was carried out in a series of papers by Khalil *et al.* [48-50]. Initially, Markov Chain Monte Carlo (MCMC) algorithms were coupled to extended Kalman filter techniques to build the joint posterior distribution of LCO amplitude of a pitching NACA0012 airfoil in the presence of noisy experimental data. More computationally efficient methods were also considered, like parallel adaptive MCMC sampling algorithms [23, 90] and Bayesian Model Selection [49, 91, 92], for the calibration of a fully-unsteady nonlinear aerodynamic model using wind-tunnel test data. Finally, the Bayesian model averaging approach was used in [73-76] to build an adjusted PAPA-based aeroelastic model from different classes of stochastic aerodynamic operator.

Problem statement

The motivation of the work presented hereafter, relies on the existence of multiple approximations of the Theodorsen [104] lift function $C(k)$, which can be considered to evaluate the unsteady aerodynamic forces acting on the pitching and plunging flat plate in an incompressible flow [33, 39, 41, 121]. Some of these approximations are given by the general form [75, 77]

$$C(k) \approx 1 - \sum_{j=1}^{N} \frac{\alpha_j k}{k - \beta_j i} \quad (14)$$

where N is the number of states of the models.

As illustrated in Table 5 and in Figure 12, several approximations can be found in the literature, depending on the number of states and the values of coefficients α_j and β_j [18, 46, 47, 89, 110].

Table 6 summarizes the experimental data of V_f^* taken from [102] and obtained for four different values of the frequency ratio ω_h / ω_α of uncoupled natural frequencies in pitch and plunge.

scenario	A	B	C	D
ω_h/ω_α	0.33	0.5	0.83	1
V_f^*	10.67	9.19	6.41	7.30

Table 6 – Experimental dataset $\mathcal{D} = \{d_A, d_B, d_C, d_D\}$ for the critical flutter velocity V_f^*, corresponding to four values of ω_h/ω_α. The other aeroelastic parameters are considered to be fixed, namely r_α = 0.5, x_α = 0.2, a_h = –0.4, μ = 400 [102].

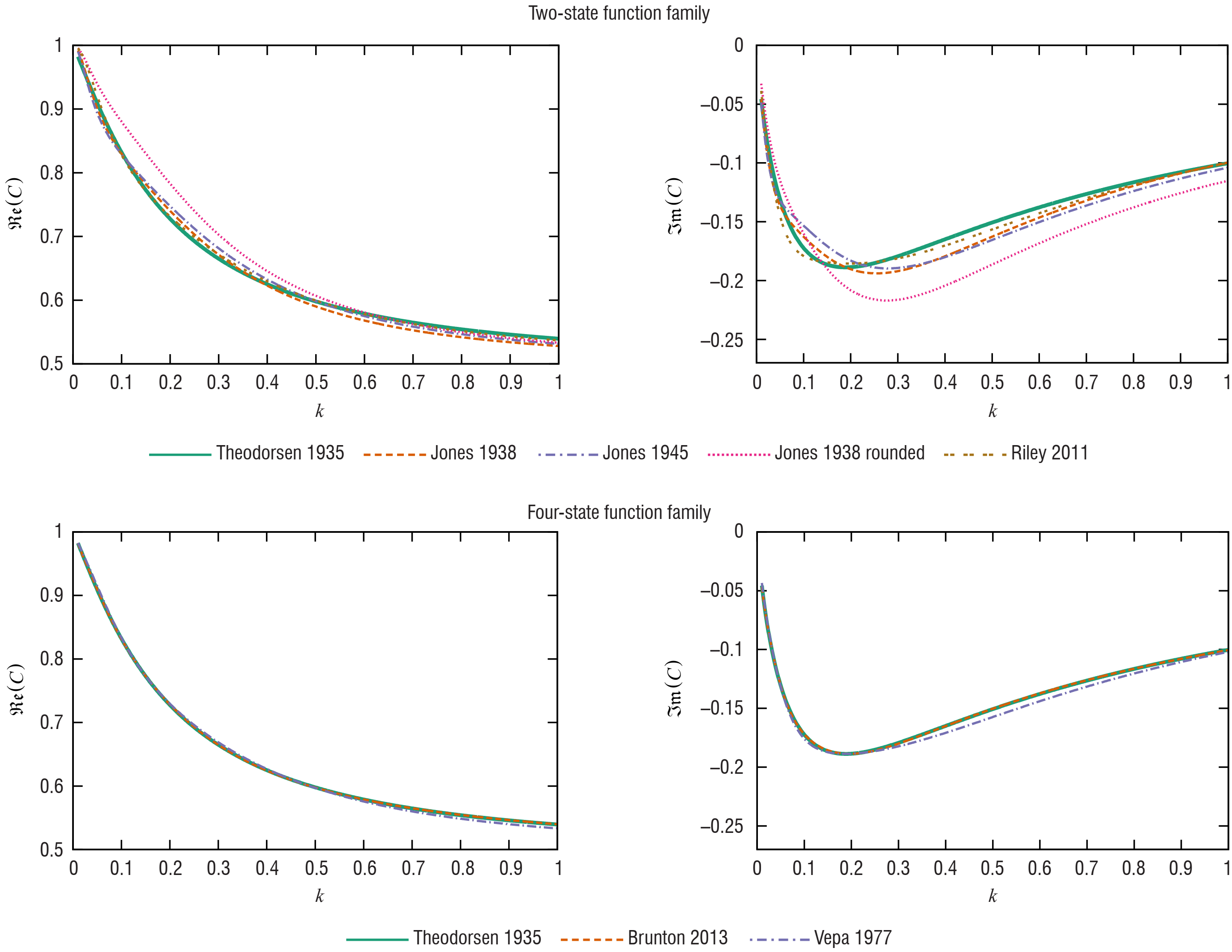

Figure 12 – Plots of typical approximations of the Theodorsen function $C(k)$ taken from [18, 75, 89] as described in Table 5.

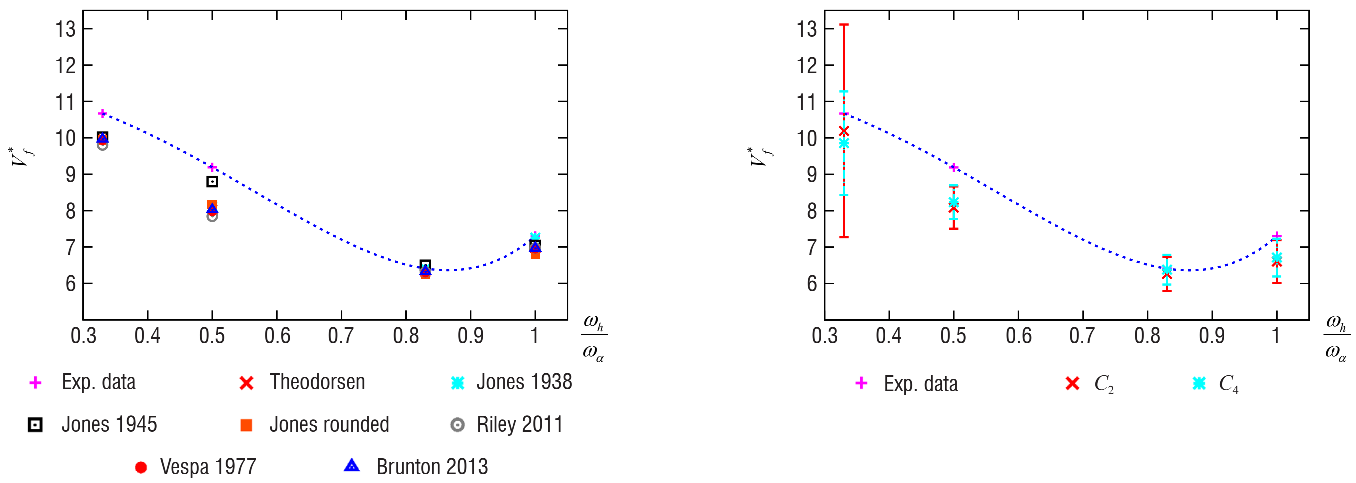

Figure 13 – Linear flutter boundary as a function of the ratio of uncoupled natural frequencies in pitch and plunge. Left: Comparison between experimental data [102] and values of the flutter speed V_f^* obtained from the approximations of the lift function $C(k)$ (Table 5). Right: Prior distributions of the model coefficients constructed according to Equation 15 using Monte Carlo sampling with 10^7 samples.

Figure 13-left shows the aeroelastic responses of a typical PAPA aeroelastic configuration, where the linear critical flutter velocity index V_f^* is computed using the iterative frequency-matching V-g method [13] for given parameters: $r_\alpha = 0.5$, $x_\alpha = 0.2$, $a_h = -0.4$, $\mu = 400$ [77]. Different spreads are observed, thus making the identification of the best approximation for all scenarios tricky.

Considering that the uncertainty associated with the choice of the more suitable model belongs to the family of epistemic model-form uncertainty, the Bayesian model averaging approach provides a theoretical framework to identify the most suited model of the lift function $C(k)$ and to calibrate its coefficients defined in Equation 14 within a stochastic framework. To this end, approximations shown in Table 5 are used to construct two stochastic models, depending on the number of states, by considering the following prior distributions for model coefficients $\tilde{\alpha}_j$ and β_j [73, 74]

$$\tilde{\alpha}_j \sim \mathcal{U}[0,1], \quad \beta_j \sim \mathcal{U}[0,0.9], \quad \tilde{\alpha}_j = \frac{\alpha_j}{\sum_{j=1}^{N} \alpha_j}, \quad j = 1,\dots,N \tag{15}$$

Figure 13-right shows the mean and the 50% maximum credibility interval of the flutter speed obtained by Monte Carlo sampling of the two stochastic models C_2 and C_4, constructed respectively using 2 and 4 states in Equation 14 and according to the prior distributions of $\tilde{\alpha}_j$ and β_j in Equation 15. The two models are driven by extreme outliers, resulting in mean values possibly outside the 50% confidence intervals. The relatively large spread of the realizations suggests that calibrations of the stochastic model might be required.

Bayesian calibration using parameter inference

Bayesian inference techniques were considered in [74, 76, 77] for the reduction of the uncertainty associated with the choice of model parameters by calibrating model coefficients of model $M_1 = C_2$ and model $M_2 = C_4$, using the available experimental observations. Let y be the output of the deterministic aeroelastic model. The quantity of interest q, corresponding to the critical flutter velocity V_f^* in the present case, is modeled as the output of the deterministic aeroelastic model y plus a random error term ε due to model inadequacy or measurement error

$$q = y(\mathbf{x}, \boldsymbol{\theta}_i, M_i) + \varepsilon(\mu_i, \sigma_i, M_i) \tag{16}$$

where $\mathbf{x}$ denotes the explicative aero-mechanical parameters and $\boldsymbol{\theta}_i$ represents the random model coefficients subject to epistemic uncertainties. The mean μ_i and the standard deviation σ_i are the hyperparameters that describe the error term ε, which is chosen to be Gaussian with zero mean [20]. Let $\mathcal{D}$ be the set of experimental data points $d_j\,(j = 1, n_d)$ of the flutter index V_f^*. The likelihood function, which corresponds to the probability of observing the data D given a model M_i, a set of parameters $\boldsymbol{\theta}_i$ and hyperparameters σ_i, is written as [8]

$$f_N(\mathcal{D}|\boldsymbol{\theta}_i, \sigma_i, M_i) = \Pi_{j=1}^{n_d} \frac{1}{\sqrt{2\pi\sigma_i^2}} \exp\left(-\frac{\left(d_j - y(\mathbf{x}_j, \boldsymbol{\theta}_i, M_i)\right)^2}{2\sigma_i^2} \right) \tag{17}$$

The joint posterior distribution of the model parameters is computed using the Bayes rule as [8]

$$p(\boldsymbol{\theta}_i, \sigma_i | \mathcal{D}, M_i) \propto f_N(\mathcal{D}|\boldsymbol{\theta}_i, \sigma_i, M_i)\, p(\boldsymbol{\theta}_i, \sigma_i | M_i) \tag{18}$$

where $p(\boldsymbol{\theta}_i, \sigma_i | M_i)$ is the joint prior probability density of the uncertain parameters and hyperparameters.

Figure 14-left presents the posterior distributions of hyperparameters whose prior distribution was taken as $p(\sigma_i|M_i) = \mathcal{U}[0.01, 0.7]$. Below values of $\sigma = 0.3$, the higher probability density values for model M_2 show that this model is able to yield more accurate results than model M_1.

Note that for $\sigma_i \to 0$, $p(\sigma|\mathcal{D}, \mathcal{M})$ vanishes, meaning that the models cannot reproduce the results without considering a discrepancy term. All computations are performed using hyperparameter inference [77], where the posterior parameter distributions for coefficient $\tilde{\beta}_1$ are presented in Figure 14-right. As expected, considering additional data leads to sharper distributions of the posterior *pdf* for the flutter speed.

Robust prediction of the stochastic models

Based on the posterior distribution of the random parameters $p(\boldsymbol{\theta}_i, \sigma_i | \mathcal{D}, M_i)$ in Equation 18, it is possible to predict an updated estimate of the quantity of interest, namely the marginal posterior predictive distribution for the critical flutter speed V_f [24]

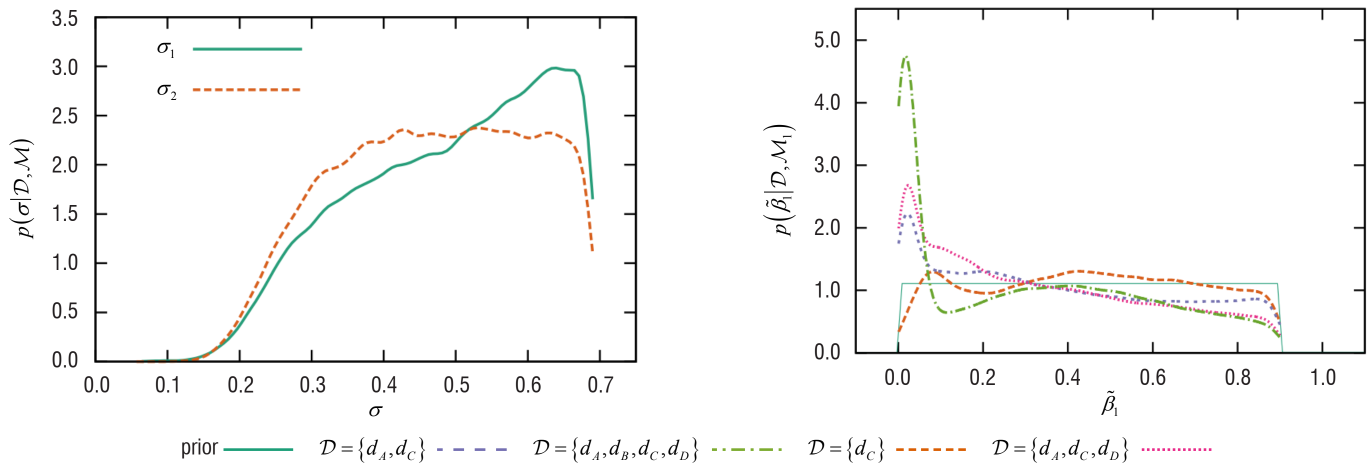

Figure 14 – Left: Kernel density estimations of the posterior distributions of σ_i for models M_1 and M_2. The prior distribution is $\sigma_i = \mathcal{U}[0.01, 0.7]$; Right: Influence of the size of the calibration dataset $\mathcal{D}$ (Table 6) on the posterior of model coefficients computed using hyperparameter inference with $\sigma_i \sim \mathcal{U}[0.01, 0.7]$.

$$p(q|\mathbf{x},\mathcal{D},M_i) = \int p(q|\mathbf{x},\boldsymbol{\theta}_i,\sigma_i,M_i)\, p(\boldsymbol{\theta}_i,\sigma_i \mid \mathcal{D},M_i)\, d\boldsymbol{\theta}_i d\sigma_i \quad (19)$$

$$\approx \frac{1}{n_s}\sum_{\ell=1}^{n_s} p(q \mid \mathbf{x},\boldsymbol{\theta}_i(\ell),\sigma_i(\ell),M_i) \quad (20)$$

where $\boldsymbol{\theta}_i(\ell)$ and $\sigma_i(\ell)$ are the ℓ-th sample of $p(\boldsymbol{\theta}_i,\sigma_i \mid \mathcal{D},M_i)$ used during the Monte Carlo integration procedure. The predictive distribution for a given set of parameters and hyperparameters $p(q \mid \mathbf{x},\boldsymbol{\theta}_i,\sigma_i,M_i)$ is defined by

$$p(q \mid \mathbf{x},\boldsymbol{\theta}_i,\sigma_i,M_i) = \frac{1}{\sqrt{2\pi\sigma_i^2}} \exp\left(-\frac{\left(q - y(\mathbf{x},\boldsymbol{\theta}_i,M_i)\right)^2}{2\sigma_i^2}\right) \quad (21)$$

Bayesian model averaging

Bayesian Model Averaging (BMA) is a statistical method [42] that accounts for the uncertainty in the selection of the model itself. The total predictive distribution $p(q \mid \mathbf{x},\mathcal{D})$ of the resulting BMA adjusted stochastic model is based on the average of the posterior predictive distributions of the two models, weighted by the posterior model probability of each individual model $\mathcal{M}_i$

$$p(q \mid \mathbf{x},\mathcal{D}) = \sum_{i=1}^{m} p(q \mid \mathbf{x},\mathcal{D},M_i)\, P(M_i \mid \mathcal{D}) \quad (22)$$

where $p(q \mid \mathcal{D},\mathbf{x},M_i)$ is the robust or posterior predictive distribution of model M_i. The posterior model probability $P(M_i \mid \mathcal{D})$ is evaluated using Bayesian inference as

$$P(M_i \mid \mathcal{D}) = \frac{P(\mathcal{D} \mid M_i)P(M_i)}{\sum_{j=1}^{m} P(\mathcal{D} \mid M_j)P(M_j)} \quad (23)$$

The prior model probability $P(M_i)$ is assumed to follow a uniform distribution. According to Cheung *et al.* [24], the marginal likelihood $P(\mathcal{D}|M_i)$ is given by

$$P(\mathcal{D}|M_i) = \int f_N(\mathcal{D}|\boldsymbol{\theta}_i,\sigma_i,M_i)\, p(\boldsymbol{\theta}_i|M_i)\, p(\sigma_i|M_i)\, d\boldsymbol{\theta}_i d\sigma_i \quad (24)$$

where the prior density $p(\boldsymbol{\theta}_i|M_i)$ is evaluated based on expert opinion.

Table 7 shows that the higher model probability is attributed to the four-state model M_2. The same conclusion holds when setting σ_i to a fixed deterministic value, or when including σ_i in the inference procedure, as described in Section "Bayesian calibration using parameter inference".

model error	$P(M_1\|\mathcal{D})$	$P(M_2\|\mathcal{D})$
$\sigma_i = 0.6$	0.3526	0.6474
$\sigma_i \sim \mathcal{U}[0.01,0.7]$	0.311	0.689

Table 7 – Posterior model probabilities $P(q|\mathbf{x},\mathcal{D},M_i)$ for calibration over $\mathcal{D} = \{d_A,d_C,d_D\}$ (Table 6) obtained from BMA with different modeling of the random error term $\varepsilon(\sigma_i,M_i)$ [77]

The total predictive distribution $p(q|\mathbf{x},\mathcal{D})_{determ.}$ for point d_B based on BMA of the deterministic (*e.g.,* non-calibrated) models, is presented in Figure 15. The most probable value for the flutter speed index is about $V_f^* \sim 8.1$, which is far from the experimental value given by $V_f^* \sim 9.19$. On the contrary, results obtained after individual

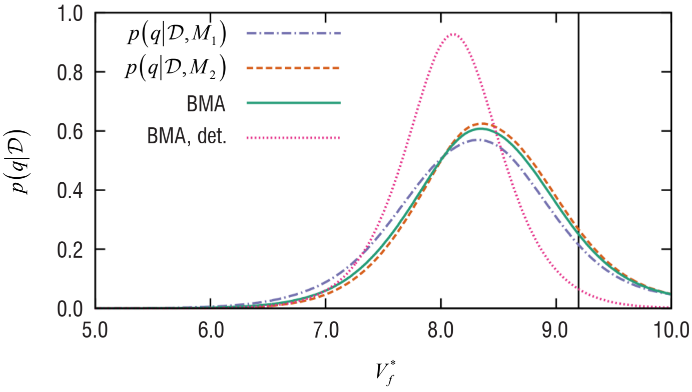

Figure 15 – Predictive distribution of the critical flutter velocity V_f^* for scenario d_B obtained by applying the BMA framework to model-form uncertainty in $C(k)$ with calibrated stochastic coefficients $\tilde{\alpha}_j$ and β_j in Equation 15 ($\mathcal{D} = \{d_A,d_C,d_D\}$ (Table 6) and $\sigma_i \sim \mathcal{U}[0.01,0.7]$ [78])

calibrations of models M_1 and M_2 over dataset $\mathcal{D} = \{d_A,d_C,d_D\}$ clearly show the benefit of calibrating the coefficients of the lift function $C(k)$, since their probability density values for the sought value of V_f^* are higher than those for the deterministic BMA.

The differences between the individual models after the Bayesian inference step are relatively small. Quite similar results are thus expected to be observed for the total predictive distribution given by BMA. Attempts were made in [77] to reduce the confidence intervals of the prediction of V_f^* by introducing a bias relative to the error term used in the Bayesian inference procedure.

Concluding remarks

This paper reviewed some recent development for the study of canonical aeroelastic systems under uncertainties. Forward stochastic analysis of parametric uncertainties in the aero-mechanical parameters were performed within the framework of Polynomial-Chaos-based approaches. Adaptive multi-element generalized Polynomial Chaos and machine learning-augmented arbitrary Polynomial Chaos were successfully used for capturing the multi-modal behavior of the stochastic critical flutter velocity or limit-cycle-oscillations. In particular, the study of variabilities in ply angles and thicknesses of composite laminate layups on the aeroelastic flutter of a cantilevered plate wing was performed. Due to the presence of a mode switch mechanism in the aeroelastic response, a dramatic reduction in the linear flutter speed was observed compared to values obtained from classical safety margins. Finally, the effects of model-form and predictive uncertainties on the flutter boundary of an elastically-mounted pitch and plunge airfoil were investigated within the framework of Bayesian uncertainty quantification. To this end, Bayesian inference was used for the stochastic calibration of the coefficients of two low-order aerodynamic models. Then, a Bayesian Model Averaging method was used to construct an adjusted stochastic model with robust predictive capabilities, where substantial reductions in the variability of the flutter boundary were obtained compared to the application of the BMA approach on deterministic aerodynamic models.

It is believed that forward uncertainty quantification in high-fidelity-based aeroelastic systems will quickly benefit from the development of advanced stochastic tools for the propagation of parametric uncertainties in canonical aeroelastic problems with discontinuous response. In particular, improvement in the prediction of the stochastic flutter boundary of complete aeroelastic aircraft configuration in the transonic flight regime are expected, by combining CFD-based aeroelastic solvers with adaptive sparse stochastic solvers [14, 87]. Although probabilistic methods are not well-suited for the accurate estimation of quantiles and probability of failure, attempts to deal with the use of polynomial chaos for robust design and the computation of failure probabilities can be found in [34, 69, 80, 104] and could be considered for reliable aeroelastic stability analysis. Moreover, variable-fidelity and multi-fidelity surrogate modeling [6, 19, 71, 95] can be used to further reduce the computation cost by combining machine learning tools and Bayesian Inference steps for the calibration of low-order aeroelastic models and observations gained from possibly CFD-based higher-fidelity models.

Due to their ability to identify or verify parameter values in the presence of model-form uncertainties, Bayesian approaches could help in constructing an adjusted stochastic model for reliable predictions of the flutter boundary. However, several issues remain to be addressed. First, the considered data sets must be sufficiently large, in order to avoid strong sensitivity of the adjusted model to the calibration data ideally, the posterior distributions should no longer vary when additional observations are added. Thus, this would lead to the construction of specially-designed aeroelastic databases for a large range of realistic scenarios. Secondly, efficient methods will be required to overcome the computational burden due to the use of CFD-based aeroelastic analysis within the Bayesian framework. To this end, surrogates based on Polynomial Chaos or stochastic collocation could be incorporated into the Bayesian inference step [3, 28, 60, 63, 105]

References

[1] B. M. ADAMS, L. E. BAUMAN, W. J. BOHNHOFF , K. R. DALBEY, M. S. EBEIDA, J. P. EDDY, M. S. ELDRED, P. D. HOUGH, K. T. HU, J. D. JAKEMAN, L. P. SWILER, D. M. VIGIL - *Dakota, a Multilevel Parallel Object-Oriented Framework for Design Optimization, Parameter Estimation, Uncertainty Quantification, and Sensitivity Analysis: Version 5.4 User's Manual*. Sandia Technical Report SAND2010-2183, December 2009. Updated April 2013, 2013.

[2] FEDERAL AVIATION ADMINISTRATION. *Aeroelastic Stability Substantiation of Transport Category Airplanes*. Advisory Circular 25.629-1B, U.S. Department of Transportation, Federal Aviation Administration, Washington, D.C., October 2014.

[3] M. ARNST, R. GHANEM, C. SOIZE - *Identification of Bayesian Posteriors for Coefficients of Chaos Expansions*. Journal of Computational Physics, 229(9):3134-3154, 2010.

[4] R. ASTER, B. BORCHERS, C. THURBER - *Parameter Estimation and Inverse Problems*. Elsevier, second edition edition, 2012.

[5] I. BABUŠKA, F. NOBILE, R. TEMPONE - *A Stochastic Collocation Method for Elliptic Partial Differential Equations with Random Input Data*. SIAM Journal on Numerical Analysis, 45(3):1005-1034, 2007.

[6] K. J. BADCOCK, S. TIMME, S. MARQUES, H. KHODAPARAST, M. PRANDINA, J. E. MOTTERSHEAD, A. SWIFT, A. DA RONCH, M. A. WOODGATE - *Transonic Aeroelastic Simulation for Instability Searches and Uncertainty Analysis*. Progress in Aerospace Sciences, 47(5):392-423, 2011.

[7] M. BAUDIN, A. DUTFOY, B. IOOSS, A.-L. POPELIN - *OpenTURNS: An Industrial Software for Uncertainty Quantification in Simulation*. Pages 1-38, Springer International Publishing, Cham, 2016.

[8] J. L. BECK, L. S. KATAFYGIOTIS - *Updating Models and their Uncertainties. I: Bayesian Statistical Framework*. Journal of Engineering Mechanics, 124:455-461, 1998.

[9] P. BERAN, B. STANFORD - *Uncertainty Quantification in Aeroelasticity*. Lecture Notes in Computational Science and Engineering, 92:59-103, 2013.

[10] P. BERAN, B. STANFORD, C. SCHROCK - *Uncertainty Quantification in Aeroelasticity*. Annual Review of Fluid Mechanics, 49(1):361-386, 2017.

[11] P. S. BERAN, C. L. PETTIT - *A Direct Method for Quantifying Limit-Cycle Oscillation Response Characteristics in the Presence of Uncertainties*. AIAA Paper 2004-1695, 2004.

[12] P. S. BERAN, C. L. PETTIT, D. R. MILLMAN - *Uncertainty Quantification of Limit-Cyle Oscillations*. Journal of Computational Physics, 217:217-247, 2006.

[13] R. L. BISPLINGHOFF, H. ASHLEY, R. L. HALFMAN, editors - *Aeroelasticity*. Addison-Wesley, 1955.

[14] G. BLATMAN, B. SUDRET - *Sparse Polynomial Chaos Expansions and Adaptive Stochastic Finite Elements using a Regression Approach*. Comptes Rendus Mécanique, 336(6):518-523, 2008.

[15] D. BORGLUND - *The $\mu - k$ Method for Robust Flutter Solutions*. Journal of Aircraft, 41(5):1209-1216, 2004.

[16] G.E.P. Box, G. C. TIAO - *Bayesian Inference in Statistical Analysis*. Wiley, 1973.

[17] L. BRUNO, C. CANUTO, D. FRANSOS - *Stochastic Aerodynamics and Aeroelasticity of a Flat Plate via Generalised Polynomial Chaos*. Journal of Fluids and Structures, 25:1158-1176, 2009.

[18] S. L. BRUNTON, C. W. ROWLEY - *Empirical State-Space Representations for Theodorsen's Lift Model*. Journal of Fluids and Structures, 38:174-186, 2013.

[19] D. E. BRYSON, M. P. RUMPFKEIL - *Variable-Fidelity Surrogate Modeling of Lambda Wing Transonic Aerodynamic Performance*. AIAA Paper No. 2016- 0294.

[20] B. P. CARLIN, T. A. LOUIS - *Bayesian Methods for Data Analysis*. Number 78 in Chapman & Hall, CRC texts in statistical science series. CRC Press, Boca Raton, Fla., 3. ed edition, 2009.

[21] J.-C. CHASSAING, D. LUCOR, J. TRÉGON - *Stochastic Nonlinear Aeroelastic Analysis of a Supersonic Lifting Surface using an Adaptive Spectral Method*. Journal of Sound and Vibration, 331:394-411, 2012.

[22] X. CHEN, Z. QIU - *A Novel Uncertainty Analysis Method for Composite Structures with Mixed Uncertainties Including Random and Interval Variables*. Composite Structures, 184:400-410, 2018.

[23] S. H. CHEUNG, J. L. BECK - *Bayesian Model Updating using Hybrid Monte Carlo Simulation with Application to Structural Dynamic Models with many Uncertain Parameters*. Journal of Engineering Mechanics, 135:243-255, 2009.

[24] S. H. CHEUNG, T. A. OLIVER, E. E. PRUDENCIO, S. PRUDHOMME, R. D. MOSER - *Bayesian Uncertainty Analysis with Applications to Turbulence Modeling*. Reliability Engineering and System Safety, 96:1137-1149, 2011.

[25] B. CHOUVION, E. SARROUY - *Development of Error Criteria for Adaptive Multi-Element Polynomial Chaos Approaches*. Mechanical Systems and Signal Processing, 66-67:201-222, 2016.

[26] M. CLYDE, E. I. GEORGE - *Model Uncertainty*. Statistical Science, 19:81-94, 2004.

[27] B. D. COLLER, P. A. CHAMARA - *Structural Non-Linearities and the Failure of the Classic Flutter Instability*. Journal of sound and vibration, 277:711-739, 2004.

[28] A. A. CONTRERAS, O. P. LE MAÎTRE, W. AQUINO, O. M. KNIO - *Multi-Model Polynomial Chaos Surrogate Dictionary for Bayesian Inference in Elasticity Problems*. Probabilistic Engineering Mechanics, 46:107-119, 2016.

[29] Y. DAI, C. YANG - *Methods and Advances in the Study of Aeroelasticity with Uncertainties*. Chinese Journal of Aeronautics, 27(3):461-474, 2014.

[30] B. P. DANOWSKY, J. R. CHRSTOS, D. H. KLYDE, C. FARHAT, M. BRENNER - *Evaluation of Aeroelastic Uncertainty Analysis Methods*. Journal of Aircraft, 47(4), 2010.

[31] J. DENG, C. ANTON, Y.S. WONG - *Uncertainty Investigations in Nonlinear Aeroelastic Systems*. Journal of Computational and Applied Mathematics, 235(13):3910-3920, 2011. Engineering and Computational Mathematics: A Special Issue of the International Conference on Engineering and Computational Mathematics, 27-29 May 2009.

[32] A. DESAI, S. SARKAR - *Uncertainty Quantification and Bifurcation Behavior of an Aeroelastic System*. ASME 2010, Paper FEDSM-ICNMM2010-30050, August 1-5, 2010 Montréal, Quebec, Canada, 2010.

[33] E. H. DOWELL, E. F. CRAWLEY, H. C. CURTISS Jr, D. A PETERS, R. H. SCANLAN, F. SISTO - *A Modern Course in Aeroelasticity.* Kluwer academic publishers edition, 1995.

[34] V. DUBOURG, B. SUDRET, F. DEHEEGER - *Metamodel-Based Importance Sampling for Structural Reliability Analysis*. Probabilistic Engineering Mechanics, 33:47-57, 2013.

[35] R. DWIGHT., H. BIJL, S. MARQUES, K. BADCOCK - *Reducing Uncertainty in Aeroelastic Boundaries Using Experimental Data*. International Forum of Aeroelasticity and Structural Dynamics, 2011.

[36] M. S. ELDRED, J. BURKARDT - *Comparison of Non-Intrusive Polynomial Chaos and Stochastic Collocation Methods for Uncertainty Quantification.* AIAA Paper No. 2009-0976, 2009.

[37] M. ESTER, H.-P. KRIEGEL, J. SANDER, X. XU - *A Density-Based Algorithm for Discovering Clusters in Large Spatial Databases with Noise.* Proceedings of the Second International Conference on Knowledge Discovery and Data Mining, volume 96, pp. 226-231, 1996.

[38] J. FEINBERG, H. P. LANGTANGEN - *Chaospy: an Open Source Tool for Designing Methods of Uncertainty Quantification*. Journal of Computational Science, 11:46-57, 2015.

[39] Y. C. FUNG - *An Introduction to the Theory of Aeroelasticity*. Dover Publications, Inc., dover edition, 1993.

[40] R. GHANEM, P. D. SPANOS - *Stochastic Finite Elements: a Spectral Approach*. Springer-Verlag, New York, 1991.

[41] D. H. HODGES, G. A. PIERCE, editors - *Introduction to Structural Dynamics and Aeroelasticity.* Cambridge University Press, 2002.

[42] J. A. HOETING, D. MADIGAN, A. E. RAFTERY, C. T. VOLINSKY - *Bayesian Model Averaging: a Tutorial*. Statistical Science, 14:382-417, 1999.

[43] S. J. HOLLOWELL, J. DUGUNDJI - *Aeroelastic Flutter and Divergence of Stiffness Coupled, Graphite/Epoxy Cantilevered Plates*. Journal of Aircraft, 21(1):69-76, January 1984.

[44] S. HOSDER, R. W. WALTERS, R. PEREZ - *A Non-Intrusive Polynomial Chaos Method for Uncertainty Propagation in CFD Simulations*. AIAA Paper 2006-891, 2006.

[45] S. HOSDER, R. W. WALTERS, M. BALCH - *Point-Collocation Nonintrusive Polynomial Chaos Method for Stochastic Computational Fluid Dynamics.* AIAA Journal, 48(12):2721-2730, 2010.

[46] R. T. JONES - *Operational Treatment of the Nonuniform-Lift Theory in Airplane Dynamics*. Technical Report 667, National Advisory Committee for Aeronautics, 1938.

[47] W. P. JONES - *Aerodynamic Forces on Wings in Nonuniform Motion.* Technical Report 2117, Aeronautical Research Council, 1945.

[48] M. KHALIL, D. POIREL, A. SARKAR - *Probabilistic Parameter Estimation of a Fluttering Aeroelastic System in The Transitional Reynolds Number Regime*. Journal of Sound and Vibration, 332:3670-3691, 2013.

[49] M. KHALIL, D. POIREL, A. SARKAR - *Bayesian Analysis of the Flutter Margin Method in Aeroelasticity*. Journal of Sound and Vibration, 384:56-74, 2016.

[50] M. KHALIL, A. SARKAR, D. POIREL - *Application of Bayesian Inference to the Flutter Margin Method: New Developments.* ASME Conference Proceedings, FEDSM-ICNMM2010-30041, 2010.

[51] N. LAMORTE, B. GLAZ, P. P. FRIEDMANN, A. J. CULLER, A.R. CROWELL, J.J. MCNAMARA - *Uncertainty Propagation in Hypersonic Aerothermoelastic Analysis.* AIAA Paper 2010-2964, 2010.

[52] J. LE MEITOUR, D. LUCOR, J.-C. CHASSAING - *Prediction of Stochastic Limit Cycle Oscillations Using an Adaptive Polynomial Chaos Method.* Journal of Aeroelasticity and Structural Dynamics, 2(1):1-20, 2010.

[53] D. LEAMER, editor - *Specification Searches*. John Wiley & Sons, 1978.

[54] B. H. K. LEE, L. Y. JIANG, Y. S. WONG - *Flutter of an Airfoil with Cubic Restoring Force*. Journal of fluids and structures, 13:75-101, 1999.

[55] B. H. K. LEE, L. LIU, K. W. CHUNG - *Airfoil Motion in Subsonic Flow with Strong Cubic Nonlinear Restoring Forces*. Journal of Sound and Vibration, 281:699-717, 2005.

[56] B. H. K. LEE, S. J. PRICE, Y. S. WONG - *Nonlinear Aeroelastic Analysis of Airfoils: Bifurcation and Chaos*. Progress in aerospace sciences, 35:205-334, 1999.

[57] L. LIBRESCU, G. CHIOCCHIA, P. MARZOCCA - *Implications of Cubic Physical/Aerodynamic Non-Linearities on the Character of The Flutter Instability Boundary*. International Journal of Non-Linear Mechanics, 38:173-199, 2003.

[58] R. LIND, M. BRENNER - *Robust Aeroservoelastic Stability Analysis: Flight-Test Applications*. Volume Chaps. 8, 9. Advances in Industrial Control, Springer-Verlag, London, 1999.

[59] M. LOKATT - *Aeroelastic Flutter Analysis Considering Modeling Uncertainties.* Journal of Fluids and Structures, 74:247-262, 2017.

[60] X. MA, N. ZABARAS - *An Efficient Bayesian Inference Approach to Inverse Problems Based on an Adaptive Sparse Grid Collocation Method*. Inverse Problems, 25(3):035013, 2009.

[61] A. MANAN, J. E. COOPER - *Prediction of Uncertain Frequency Response Function Bounds using Polynomial Chaos Expansion.* Journal of Sound and Vibration, 329(16):3348-3358, 2010.

[62] S. MARELLI , B. SUDRET - *UQLab: A Framework for Uncertainty Quantification in Matlab*. Vulnerability, Uncertainty, and Risk, Proc. 2nd Int. Conf. on Vulnerability, Risk Analysis and Management (ICVRAM2014), Liverpool, United Kingdom, 2554-2563, 2014.

[63] Y. M. MARZOUK, H. N. NAJM - *Dimensionality Reduction and Polynomial Chaos Acceleration of Bayesian Inference in Inverse Problems*. Journal of Computational Physics, 228(6):1862-1902, 2009.

[64] R. E. MELCHERS - *Structural Reliability Analysis and Predictions*. Wiley, New York, 1999.

[65] D. R. MILLMAN - *Quantifying Initial Conditions and Parametric Uncertainties in a Nonlinear Aeroelastic System With an Efficient Stochastic Algorithm*. Technical report, PhD. Dissertation, Air Force Institute of Technology, september 2004.

[66] D. R. MILLMAN, P. I. KING, P. S. BERAN - *Airfoil Pitch-and-Plunge Bifurcation Behavior with Fourier Chaos Expansions*. Journal of Aircraft, 42(2):376-384, 2005.

[67] M. D. MINICH, C. C. CHAMIS - *Analytical Displacements and Vibrations of Cantilevered Unsymmetric Fiber Composite Laminates.* AIAA, ASME, and SAE, Structures, Structural Dynamics, and Materials Conference, Denver, Colorado, January 1975.

[68] J. P. MURCIA, P.-E. RÉTHORÉ, N. DIMITROV, A. NATARAJAN, J. D. SØRENSEN, P. GRAF, T. KIM - *Uncertainty Propagation through an Aeroelastic Wind Turbine Model using Polynomial Surrogates*. Renewable Energy, 119:910-922, 2018.

[69] V. NAIR, S. SARKAR, R. I. SUJITH - *Uncertainty Quantification of Subcritical Bifurcations*. Probabilistic Engineering Mechanics, 34:177-188, 2013.

[70] M. NAVARRO, J. WITTEVEEN, J. BLOM - *Polynomial Chaos Expansion for General Multivariate Distributions with Correlated Variables*. Technical report, Centrum Wiskunde & Informatica, 2014.

[71] L. W. T. NG, M. S. ELDRED - *Multifidelity Uncertainty Quantification using Non-Intrusive Polynomial Chaos and Stochastic Collocation*. 53rd AIAA Structures, Structural Dynamics, and Materials Conference, AIAA, pp. 1-17, April 2012.

[72] M. NIKBAY, P. ACAR - *Robust Aeroelastic Design Optimization of Wing/Store Configurations Based on Flutter Criteria*. 14th AIAA/ISSMO Multidisciplinary Analysis and Optimization (MAO) Conference, September 2012.

[73] C. NITSCHKE - *Quantification of Aleatory and Epistemic Uncertainties in the Prediction of Aeroelastic Instabilities*. PhD thesis, UNIVERSITÉ PIERRE ET MARIE CURIE, Feb. 2018.

[74] C. T. NITSCHKE, J.-C. CHASSAING - *Acceleration of Bayesian Calibration for Predictive Uncertainty Quantification in Aeroelastic Flutter.* ECCOMAS Congress, June 5-10, Creete, Greece, 2016.

[75] C. T. NITSCHKE, J.-C. CHASSAING, P. CINNELLA, D. LUCOR - *Quantification of Model-Form Uncertainty in Nonlinear Aeroelasticity.* WCCM XI, Barcelona, Spain, 20-25 July, 2014.

[76] C. T. NITSCHKE, J.-C. CHASSAING, P. CINNELLA, D. LUCOR - *Bayesian Calibration and Uncertainty Analysis for Airfoil Flutter Predictions*. UNCECOMP 2015, 25-27 May, Crete Island, Greece, 2015.

[77] C. T. NITSCHKE, P. CINNELLA, D. LUCOR, J.-C. CHASSAING - *Model-Form and Predictive Uncertainty Quantification in Linear Aeroelasticity*. Journal of Fluids and Structures, 73:137-161, 2017.

[78] C. T. NITSCHKE, A. VINCENTI, J.-C. CHASSAING - *Uncertainty Quantification in the Vicinity of Mode Switches in the Flutter Response of a Composite Cantilevered Wing*. International Forum on Aeroelasticity and Structural Dynamics, IFASD 2017, 25-28 June 2017 Como, Italy, 2017.

[79] S. OLADYSHKIN, W. NOWAK - *Data-Driven Uncertainty Quantification using the Arbitrary Polynomial Chaos Expansion*. Reliability Engineering and System Safety, 106:179-190, 2012.

[80] M. PAFFRATH, U. WEVER - *Adapted Polynomial Chaos Expansion for Failure Detection*. Journal of Computational Physics, 226(1):263-281, 2007.

[81] I. PARK, H. K. AMARCHINTA, R. V. GRANDHI - *A Bayesian Approach for Quantification of Model Uncertainty*. Reliability Engineering and System Safety, 95:777-785, 2010.

[82] J. A. PAULSON, E. A. BUEHLER, A. MESBAH - *Arbitrary Polynomial Chaos for Uncertainty Propagation of Correlated Random Variables in Dynamic Systems*. IFAC-PapersOnLine, 50(1):3548-3553, 20th IFAC World Congress, 2017.

[83] F. PEDREGOSA, G. VAROQUAUX, A. GRAMFORT, V. MICHEL, B. THIRION, O. GRISEL, M. BLONDEL, P. PRETTENHOFER, R. WEISS, V. DUBOURG, J. VANDERPLAS, A. PASSOS, D. COURNAPEAU, M. BRUCHER, M. PERROT, E. DUCHESNAY - *Scikit-learn: Machine Learning in Python*. Journal of Machine Learning Research, 12:2825-2830, 2011.

[84] C. L. PETTIT - *Uncertainty Quantification in Aeroelasticity: Recent Results and Research Challenges*. Journal of Aircraft, 41:1217-1229, 2004.

[85] C. L. PETTIT, P. S. BERAN - *Effects of Parametric Uncertainty on Airfoil Limit Cycle Oscillation*. Journal of Aircraft, 40(5):1004-1006, 2003.

[86] V. M. RAO, A. BEHAL, P. MARZOCCA, C. M. RUBILLO - *Adaptative Aeroelastic Vibration Suppression of a Supersonic Airfoil With Flap*. Aerospace Science and Technology, 10:309-315, 2006.

[87] A. RESMINI, J. PETER, D. LUCOR - *Sparse Grids-Based Stochastic Approximations with Applications to Aerodynamics Sensitivity Analysis*. International Journal for Numerical Methods in Engineering, 106(1):32-57, 2016.

[88] M. E. RILEY, R. V. GRANDHI - *Quantification of Model-Form and Predictive Uncertainty for Multi-Physics Simulation.* Computers and Structures, 89:1206-1213, 2011.

[89] M. E. RILEY - *Quantification of Model-Form, Predictive, and Parametric Uncertainties in Simulation-Based Design*. PhD thesis, Wright State University, 2011.

[90] R. SANDHU, M. KHALIL, A. SARKAR, D. POIREL - *Bayesian Model Selection for Nonlinear Aeroelastic Systems using Wind-Tunnel Data*. Computer Methods in Applied Mechanical Engineering, 282:161-183, 2014.

[91] R. SANDHU, C. PETTIT, M. KHALIL, D. POIREL, A. SARKAR - *Bayesian Model Selection using Automatic Relevance Determination for Nonlinear Dynamical Systems*. Computer Methods in Applied Mechanics and Engineering, 320:237-260, 2017.

[92] R. SANDHU, D. POIREL, C. PETTIT, M. KHALIL, A. SARKAR - *Bayesian Inference of Nonlinear Unsteady Aerodynamics from Aeroelastic Limit Cycle Oscillations*. Journal of Computational Physics, 316:534-557, 2016.

[93] S. SARKAR, J. A. S. WITTEVEEN, A. LOEVEN, H. BIJL - *Effect of Uncertainty on the Bifurcation Behavior of Pitching Airfoil Stall Flutter.* Journal of Fluids and Structures, 25(2):304-320, 2009.

[94] C. SCARTH, J. E. COOPER, P. M. WEAVER, G.H.C. SILVA - *Uncertainty Quantification of Aeroelastic Stability of Composite Plate Wings using Lamination Parameters*. Composite Structures, 116:84-93, September 2014.

[95] H. SHAH, S. HOSDER, S. KOZIEL, Y. A. TESFAHUNEGN, L. LEIFSSON - *Multi-Fidelity Robust Aerodynamic Design Optimization under Mixed Uncertainty*. Aerospace Science and Technology, 45:17-29, 2015.

[96] I. M. SOBOL - *Global Sensitivity Indices for Nonlinear Mathematical Models and their Monte Carlo Estimates.* Mathematics and Computers in Simulation, 55:271-280, 2001.

[97] C. SOIZE, R. GHANEM - *Physical Systems with Random Uncertainties: Chaos Representations with Arbitrary Probability Measure*. SIAM Journal on Scientific Computing, 26(2):395-410, January 2004.

[98] B. K. STANFORD, S. J. MASSEY - *Uncertainty Quantification of the Fun3d-Predicted Nasa Crm Flutter Boundary*. AIAA Paper No. AIAA-2017-1816, 2017.

[99] O. STODIECK, J. E. COOPER, P. M. WEAVER, P. KEALY - *Improved Aeroelastic Tailoring Using Tow-Steered Composites.* Composite Structures, 106:703-715, December 2013.

[100] M. A. TATANG, W. PAN, R. G. PRINN, G. J. MCRAE - *An Efficient Method for Parametric Uncertainty Analysis of Numerical Geophysical Model*. Journal of Geophysical Research Atmospheres, 102(18):21925-21932, September 1997.

[101] M. T. THANUSHA, S. SARKAR - *Uncertainty Quantification of Subcritical Nonlinear Aeroelastic System using Integrated Interpolation Method and Polynomial Chaos Expansion*. Procedia Engineering, 144:982-989, 2016. International Conference on Vibration Problems 2015.

[102] T. THEODORSEN - *General Theory of Aerodynamic Instability and the Mechanism of Flutter.* Technical Report 496, National Advisory Committee for Aeronautics, 1935.

[103] J. P. THOMAS, E. H. DOWELL, K. C. HALL - *An Investigation of the Sensitivity of F-16 Fighter Flutter Onset and Limit Cycle Oscillations to Uncertainties*. Volume 5 of AIAA/ASME/ASCE/AHS/ASC Structures, Structural Dynamics and Materials Conference, pp. 3137-3144, 2006.

[104] A. J. TORII, R. H. LOPEZ, L. F. F. MIGUEL - *Probability of Failure Sensitivity Analysis using Polynomial Expansion.* Probabilistic Engineering Mechanics, 48:76-84, 2017.

[105] H. A. TRAN, C. G. WEBSTER, G. ZHANG - *A Sparse Grid Method for Bayesian Uncertainty Quantification with Application to Large Eddy Simulation Turbulence Models.* ArXiv e-prints, 2015.

[106] S. W. TSAI, H. T. HAHN - *Introduction to Composite Materials*. Technomic Publ, Lancaster, Pa., 1980.

[107] U.S. DEPARTMENT OF DEFENSE - *Composite Materials Handbook.* U.S. Department of Defense, June 2002.

[108] P. VANNUCCI - *Plane Anisotropy by the Polar Method*. Meccanica, 40(4-6):437-454, December 2005.

[109] J. C. VASSBERG, M. A. DEHAAN, S. M. RIVERS, R. A. WAHLS - *Development of a Common Research Model for Applied CFD Validation Studies.* AIAA Paper No. 2008-6919, 2008.

[110] R. VEPA - *Finite State Modeling of Aeroelastic Systems.* Technical Report CR-2779, National Aeronautics and Space Administration, Langley Research Center, 1977.

[111] G. VERCHERY - *Les invariants des tenseurs d'ordre 4 du type de l'élasticité.* Comportement Méchanique des Solides Anisotropes, Volume 115, pp. 93-104, Villard-de-Lans, 1979. Éditions du CNRS, Paris.

[112] R. W. WALTERS - *Towards Stochastic Fluid Mechanics via Polynomial Chaos*. AIAA Paper 2003-413, 2003.

[113] X. WAN, G. E. KARNIADAKIS - *An Adaptive Multi-Element Generalized Polynomial Chaos Method for Stochastic Differential Equations.* Journal of Computational Physics, 209:617-642, 2005.

[114] X. WAN, G. E. KARNIADAKIS - *Multi-Element Generalized Polynomial Chaos for Arbitrary Probability Measures*. SIAM Journal of Scientific Computing, 28(3):901-928, 2006.

[115] N. WIENER - *The Homogeneous Chaos*. American Journal of Mathematics, 60(4):pp. 897-936, 1938.

[116] J. A. S. WITTEVEEN, H. BIJL - *An Alternative Unsteady Adaptive Stochastic Finite Elements Formulation based on Interpolation at Constant Phase*. Computer Methods in Applied Mechanics and Engineering, 198(3-4):578-591, 2008.

[117] J. A. S. WITTEVEEN, H. BIJL - *An Unsteady Adaptative Stochastic Finite Elements Formulation for Rigid-Body Fluid-Structure Interaction*. Computers and Structures, 86:2123-2140, 2008.

[118] J. A. S. WITTEVEEN, H. BIJL - *A Tvd Uncertainty Quantification Method with Bounded Error Applied to Transonic Airfoil Flutter*. Communications in Computational Physics, 6:406-432, 2009.

[119] J. A. S. WITTEVEEN, A. LOEVEN, S. SARKAR, H. BIJL - *Probabilistic Collocation for Period-1 Limit Cycle Oscillations*. Journal of Sound and Vibration, 311(311):421-439, 2008.

[120] J. A. S. WITTEVEEN, S. SARKAR, H. BIJL - *Modeling Physical Uncertainties in Dynamic Stall Induced Fluid-Structure Interaction of Turbine Blades Using Arbitrary Polynomial Chaos*. Computers and Structures, 85(11):866-878, 2007. Fourth MIT Conference on Computational Fluid and Solid Mechanics.

[121] J. R. WRIGHT, J. E. COOPER - *Introduction to Aircraft Aeroelasticity and Loads*. Wiley, Chichester, 2. ed edition, 2015.

[122] C. WU, H. ZHANG, T. FANG - *Flutter Analysis of an Airfoil with Bounded Random Parameters in Compressible Flows via Gegenbauer Polynomial Approximation.* Aerospace Science and Technology, 11:518-526, 2007.

[123] D. XIU, G. E. KARNIADAKIS - *The Wiener-Askey Polynomial Chaos for Stochastic Differential Equations.* SIAM Journal on Scientific Computing, 24:619-644, 2002.

[124] D. XIU, J. S. HESTHAVEN - *High-Order Collocation Methods for Differential Equations with Random Inputs.* SIAM Journal on Scientific Computing, 27(3):1118-1139, 2005.

[125] J. Y. GAN, H.-S. IM, X. Y. CHEN, G.-C. ZHA, C. L. PASILIAO - *Delayed Detached Eddy Simulation of Wing Flutter Boundary using High Order Schemes*. Journal of Fluids and Structures, 71(Supplement C):199-216, 2017.

[126] Z. ZHANG, S. YANG, F. LIU, D.M. SCHUSTER - *Prediction of Flutter and LCO by an Euler Method on Non-Moving Cartesian Grids with Boundary-Layer Corrections.* AIAA Paper 2005-0833.

Jean-Camille Chassaing received his M.S. degree in fluid mechanics from the *Ecole Nationale Supérieure d'Ingénieurs de Constructions Aéronautiques* (Toulouse, France) in 1997. He obtained a PhD degree in mechanical engineering from the *Université Pierre et Marie Curie* in 2002. After a postdoctoral stay at the Vibration University Technology Centre of the Imperial College in 2003, he was given an academic position as Assistant Professor at the *Université Pierre et Marie Curie* (France). He obtained his accreditation to supervise research (*Habilitation à Diriger des Recherches*) in 2012 in the field of uncertainty quantification in aeroelasticity and took part in the French research project CAPCAO, dedicated to the development of fast methods for the prediction of turbomachinery flutter. His research interests include fluid–structure interactions, probabilistic aeroelasticity, data assimilation and high-order numerical methods for computational fluid dynamics. He is currently an Full Professor at the Institute Jean Le Rond d'Alembert of the Sorbonne University and associate editor of the Mechanics & Industry Journal.

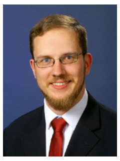

Christian Nitschke is a postdoc researcher in mechanics and applied mathematics at Paul Sabatier University in Toulouse. He graduated in mechanics from a double Master program at Karlsruhe Institute of Technology and *Arts et Métiers ParisTech* in 2015. At the beginning of 2018, he obtained a PhD degree at Sorbonne University for his work on the quantification of aleatory and epistemic uncertainties in aeroelasticity. He then returned to *Arts et Métiers ParisTech*, where he further developed his work on combined uncertainty quantification problems. Currently, Christian Nitschke works at the Clément Ader Institute in Toulouse, where he is investigating applications of artificial intelligence in the prediction of material fatigue. Throughout his career, he has been invested in questions of the use of data in engineering applications, especially within the context of machine learning and uncertainty quantification.

Didier Lucor is currently a research director at the French National Research Agency (CNRS) who received his MSc (2000) and PhD (2004) degrees in applied mathematics from Brown University, USA, under the supervision of Prof. G. Em Karniadakis. He was a postdoctoral fellow (2004-2005) in the department of Ocean Engineering at MIT, in the USA. He has received a French national award "*Chaires d'Excellence*" and funding from French Ministry of Research (2004). He was given a permanent position as fluid mechanics research scientist at the CNRS (2005), at the d'Alembert Institute of the *Université Pierre et Marie Curie* (UPMC) in Paris, France. He has been yearly involved with teaching at MSc and BSc levels at the UPMC (since 2005), and was an elected member of the UPMC governing board (2012-2015). He obtained his accreditation to supervise research (*Habilitation à Diriger des Recherches*) at the UPMC (2011). He became a senior research scientist at the CNRS (2015), and moved to the Computer Science Laboratory for Mechanics and Engineering Sciences (LIMSI) in Orsay, France. He is the coordinator of the special interest group on Uncertainty Quantification of ERCOFTAC. His research and teaching activities are related to the fields of predictive and stochastic modeling in computational mechanics, uncertainty quantification, data assimilation and robust optimization with particular focus on fluid-structure interaction problems with applications in biofluids, aerodynamics or environmental flows.

Paola Cinnella is a full professor in Fluid Mechanics at *Ecole Nationale Supérieure d'Arts et Métiers* (ENSAM), France. She graduated *summa cum laude* in Mechanical Engineering from the *Politecnico di Bari* (Italy) in 1995. In 1999, she obtained a PhD degree in Fluid Mechanics (summa cum laude) from ENSAM, where she also worked as a lecturer in Fluid Dynamics, from 1999 to 2000. After a postdoc at *Politecnico di Bari* (2000-2001), she joined the Faculty at the University of Salento (Italy) as an Assistant Professor from 2001 to 2008. In September 2008, she moved back to Paris, after obtaining a position of full professor at ENSAM. She has been a member of the Fluid Dynamics Laboratory (DynFluid) since then. She was the Head of DynFluid from 2011 to 2013. She was also the chairman of the Master of Science "Fluids and Energy Systems" program from 2010 to 2013, and a member of the Scientific Board of ENSAM from 2013 to 2017. She is the Vice-President of the board of directors of *Arts et Métiers ParisTech* since January 2018. P. Cinnella has been doing research for more than 20 years on high-fidelity methods for Computational Fluid Dynamics (CFD), focusing on high-order numerical schemes for compressible flows and uncertainty quantification. She has published more than 100 scientific papers, mostly peer-reviewed journal articles or international conference proceedings. She has been the investigator or principal investigator in many research projects in France and in Italy, including the FP7 project IDIHOM (industrialization of high-order methods) and the French projects UFO (Uncertainty quantification for flow optimization) and TRENERGY (TRain ENergy Efficiency via Rankine-cycle exhaust Gas heat recovery, involving a task in uncertainty quantification and robust optimization). She supervises or has supervised 20 PhD candidates and about 45 Master of Science candidates.

She has given invited lectures in the USA, France, Italy, the Netherlands, and Chile. She is a member of several scientific committees of international conferences and a referee for most major journals and conferences in CFD. She is a member of the Aerodynamics Panel of the French Association of Aeronautics and Astronautics.

Angela Vincenti is an Associate Professor in Solid and Structural Mechanics at the Sorbonne University, in Paris (France). She graduated in Mechanical Engineering from the *Università di Pisa* (Italy) in 1999, and in 2002 she obtained a PhD in Mechanics at the *Université de Bourgogne* (France) with her work on the optimization of composite laminates. After a one-year post-doctoral position at the University of Reading (UK) working on the design of composite structures, and a short research experience at BOKU University in Vienna (Austria) studying the mechanical behavior of wood glued assemblies, she joined the *Université Pierre et Marie Curie* (Paris 6, former name of the Sorbonne University) in September 2004 as Assistant Professor and was confirmed as Associate Professor in 2005. She is a member of the *Institut d'Alembert*, the research institute in Mechanics at the Sorbonne University. She teaches courses in solid and structural mechanics, composite materials and optimization at the Sorbonne University. Her research activities are related to the development of advanced methods for the design and optimization of composite materials and structures, both in the linear and nonlinear domains. Her recent projects have been focused on the study of multistable structures (she obtained the Young-Researcher grant from the *Agence Nationale de la Recherche* in 2013) and aeroelastic behavior of composite aeronautical structures.